

UPDATED REFERENCE DESIGN OF A LIQUID METAL COOLED  
TANDEM MIRROR FUSION BREEDER

D.H. Berwald, R.H. Whitley, J.K. Garner,  
R.J. Gromada, T.J. McCarville

TRW, Inc., Redondo Beach, CA 90278

R.W. Moir, J.D. Lee, B.R. Bandini, F.J. Fulton  
Lawrence Livermore National Laboratory  
Livermore, CA 94550

C.P.C. Wong, I. Maya, C.G. Hoot, K.R. Schultz  
GA Technologies, Inc., San Diego, CA 92138

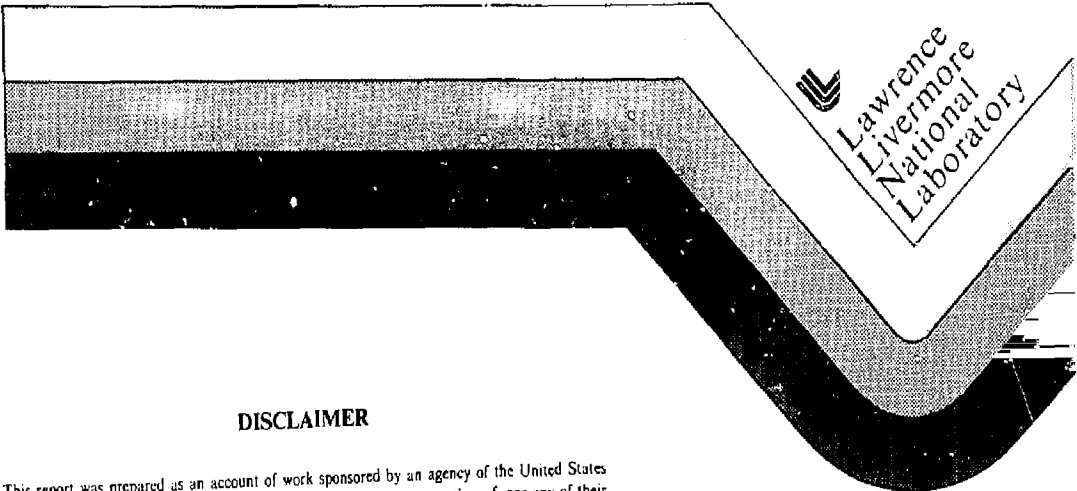
L.G. Miller, J.M. Beeston, B.L. Harris  
Idaho National Engineering Laboratory (INEL-EG&G)  
Idaho Falls, ID 83401

R.A. Westman, N.M. Ghoniem, G. Orient  
University of California, Los Angeles  
Los Angeles, CA 90024

H. Wolfer  
University of Wisconsin-Madison, WI 53706

J.H. DeVan, P. Torterelli  
Oak Ridge National Laboratory  
Oak Ridge, TN 37830

September, 1985



**DISCLAIMER**

This report was prepared as an account of work sponsored by an agency of the United States Government. Neither the United States Government nor any agency thereof, nor any of their employees, makes any warranty, express or implied, or assumes any legal liability or responsibility for the accuracy, completeness, or usefulness of any information, apparatus, product, or process disclosed, or represents that its use would not infringe privately owned rights. Reference herein to any specific commercial product, process, or service by trade name, trademark, manufacturer, or otherwise does not necessarily constitute or imply its endorsement, recommendation, or favoring by the United States Government or any agency thereof. The views and opinions of authors expressed herein do not necessarily state or reflect those of the United States Government or any agency thereof.

**MASTER**

DISTRIBUTION OF THIS DOCUMENT IS UNLIMITED

UPDATED REFERENCE DESIGN OF A LIQUID METAL COOLED  
TANDEM MIRROR FUSION BREEDER

D. H. Berwald, R. H. Whitley, J. K. Garner,  
R. J. Gromada, T. J. McCarville  
TRW, Inc. Redondo Beach, CA 90278

R. W. Moir, J. D. Lee, B. R. Bandini, F. J. Fulton,  
Lawrence Livermore National Laboratory,  
Livermore, CA. 94550

C. P. C. Wong, I. Maya, C. G. Hoot, K. R. Schultz,  
GA Technologies, Inc.  
San Diego, CA 92138

L. G. Miller, J. M. Beeston, B. L. Harris,  
Idaho National Engineering Laboratory (INEL-EG&G)  
Idaho Falls, ID 83401

R. A. Westman, N. M. Ghoniem, G. Orient,  
University of California, Los Angeles,  
Los Angeles, CA 90024

M. Wolfer,  
University of Wisconsin Madison,  
Wisconsin 53706

J. H. DeVan, P. Tortorelli,  
Oak Ridge National Laboratory  
Oak Ridge, TN 37830

September, 1985

## ABSTRACT

Detailed studies of key technical issues for liquid metal cooled fusion breeder (fusion-fission hybrid blankets) have been performed during the period 1983-4. Based upon the results of these studies, the 1982 reference liquid metal cooled tandem mirror fusion breeder blanket design was updated and is described. The updated reference blankets provides increased breeding and lower technological risk in comparison with the original reference blanket. In addition to the blanket design revisions, a plant concept, cost, and fuel cycle economics assessment is provided. The fusion breeder continues to promise an economical source of fissile fuel for the indefinite future.

## TABLE OF CONTENTS

<u>SECTION</u>		<u>PAGE</u>
I.	INTRODUCTION	
I.A.	Motivation	1
I.B.	Fusion Breeder Design Development	2
I.C.	Tandem Mirror Fusion Driver Overview	4
I.D.	Fusion Breeder Design Approach & Concept Selection	4
II.	DESIGN OVERVIEW	
II.A.	Design Description	8
II.B.	Blanket Materials Selection	15
III.	KEY DESIGN AREAS	
III.A.	Nuclear Design and full management	22
III.B.	Liquid Metal Coolant Flow	28
III.B.1	Packed Bed Pressure Drop	30
III.B.2	Pressure Drop Summary	35
III.C.1	Structural Design Requirements and design features	37
III.C.2	Stress Modeling	38
III.D	Beryllium/Thorium Pebble Fuel Element	47
III.D.1	Beryllium Resources	49
III.D.2	Pebble Design Considerations	49
III.D.3	Beryllium Lifetime	56
III.E	Reactor Safety	58
III.E.1	Safety Requirements and goals	59
III.E.2	Safety Issues, Design Features & Subsystems	60
III.E.2.a	Nuclear Reactivity/Criticality	60
III.E.2.b	Pebble Expansion	61
III.E.2.c	Lithium Fire	61
III.E.2.d	Nuclear Decay Afterheat	62
III.E.3	Safety Systems Modeling	65
III.E.4	Results of Probabilistic Risk Assessment	68
IV.	FUSION BREEDER PLANT CONCEPT	
IV.A	Plant Overview	72
IV.B	Integrated Power Flow Summary	74
IV.C	Plant Cost Estimate	77
V.	FUEL CYCLE TECHNOLOGIES	
V.A	Fusion Breeder Fuel Reprocessing Issues	84
V.B	Overview of LWR Fuel Cycles and Issues	87
V.C	Symbiotic Electricity Generation Systems	90

TABLE OF CONTENTS (continued)

<u>SECTION</u>		<u>PAGE</u>
VI.	ECONOMICS	
VI.A	System Average Capital Cost Model	94
VII.B	Higher Level Economics Modeling	95
VII.B.1	Discussion	95
VII.B.2	U <sub>3</sub> O <sub>8</sub> Fueled LWR	97
VII.8.3	Economics Results for the Symbiotic System	99
VIII	Research Needs	103
IX	References	104

## I. INTRODUCTION

### I.A. Motivation

If nuclear fission takes its logical place in the United States and world's energy mix, a shortfall in uranium resources will become a real possibility in the middle of the next century.<sup>(1)</sup> Fusion could alleviate this shortfall by producing fissile fuels via the transmutation of abundant fertile materials such as  $^{238}\text{U}$  and  $^{232}\text{Th}$ . Fusion reactors which utilize fusion neutrons in this manner are designated "fusion breeders." The often used term "fusion-fission hybrid" is roughly synonymous, but also includes very high blanket energy multiplication systems, which would be optimized for in-situ power production.

Fusion breeders optimized to emphasize fissile fuel production would replace the uranium mining and enrichment segments of the fission fuel cycle and would enable the continued use of fission converter reactors such as those currently in use. Studies indicate that each fusion breeder nevertheless can provide an economical source of fissile fuel to support 10 to 15 times as many fission reactors of the same rated (thermal) power <sup>(2,3,4)</sup>. Because relatively few fusion breeders would be needed to support a rather large nuclear fission capacity, it is not likely that a fusion breeder would be owned by an individual utility. Rather, one or more fusion breeders would be located in a dedicated fuel cycle center including all of the required fuel processing facilities (e.g., reprocessing, fabrication). The fuel cycle center would be owned and operated by an industrial concern (e.g., a consortium of utilities) or under the auspices of the federal government (as uranium enrichment plants are owned and operated today).

Based upon the many studies which have been performed, it is our opinion

that a marriage of fusion and fission via the fusion breeder can result in the earliest large scale application of nuclear fusion. This option is not resource limited for the foreseeable future, but could be replaced by fusion-electric power generation should the latter application become economically viable. The early development of fusion breeder reactors will encourage the later development of the more challenging fusion-electric reactors by providing an industrial base as well as operating experience.

### I.B. Fusion Breeder Design Development

The design of fusion breeders has progressed to a level of conceptual detail which requires a multidisciplinary team approach. The study reported here has included the participation of the following organizations:

<u>Organization</u>	<u>Principal Responsibilities</u>
Lawrence Livermore National Laboratory	Program Management, Tandem Mirror Physics and Technology, Nuclear Data and Design, Beryllium Fabrication, Pyrochemical Reprocessing
TRW, Inc.	Design Coordination and Integration, Tandem Mirror Plasma and Systems Engineering, Liquid Metal MHD Flow, Fuel Cycle and Economics

GA Technologies, Inc. Fluid Mechanics and Heat  
Transfer,  
Fuel Handling Systems,  
Reactor Safety Systems,

Westinghouse Electric Mechanical Design,  
Company  
Reactor System Layout

Oak Ridge Chemical Engineering and  
National Laboratory Materials Compatibility

Idaho National Beryllium Performance  
Engineering Laboratory

In addition, investigators from the University of California at Los Angeles (structural mechanics and ferritic steel irradiation damage), the University of Wisconsin (beryllium irradiation damage) and the Energy Technology Engineering Center (liquid metals and materials) participated in the study.

Several detailed laboratory reports relating to the evolution of a reference liquid metal cooled tandem mirror fusion breeder design concept have been issued. (2,5,6,7,8,9) Reference 2 is the most complete description of the design, but is updated by Reference 5, which is devoted to more detailed studies of key engineering issues. References 8 and 9 primarily relate to the use of beryllium in fusion applications. In this report, the results of these prior studies have been synthesized to best represent a "reference" liquid metal cooled fusion breeder reactor. Helium cooled tokamak and tandem

mirror fusion breeders have also been considered in design studies. (3,4)

#### I.C. Tandem Mirror Fusion Driver Overview

The fusion driver for the reference tandem mirror fusion breeder is nearly identical to the fusion driver design concept developed for the Mirror Advanced Reactor Study (MARS).<sup>(10)</sup> It should be noted that the goal of achieving economic breakeven for a fusion breeder which competes with mined and enriched uranium fuel for LWRs requires a level of plasma performance approaching that of the MARS and Starfire fusion electric designs <sup>(10,11)</sup> More recent studies (e.g., MINIMARS) recognize that fusion-electric reactor performance must exceed that of MARS or Starfire to be economically attractive. (12,13)

The MARS fusion driver is well documented and will not be described in detail. Table I provides a brief summary of its features. Reference 10 provides a detailed description.

#### I.D. Fusion Breeder Design Approach and Concept Selection

A principal goal of the design study has been to develop an improved understanding of technology requirements for unique components of the fusion breeder/and its fuel cycle, thus eliminating technological "blind alleys". These components include the breeding blanket, the primary loop, the fuel handling systems, reactor safety systems and any unique fuel cycle facilities (e.g., fuel reprocessing, fuel fabrication).

The reference tandem mirror blanket is of the "fission-suppressed" class, in which non-fission nuclear reactions [ $\text{Be}(n,2n)$  and  ${}^7\text{Li}(n,n'\text{T})$ ] are used to generate excess neutron multiplication beyond that required to sustain tritium self-sufficiency. This class of blanket has been emphasized in recent studies

Table I.

## Major Parameters for the MARS Fusion Driver

Central cell length	130 m
Plasma radius	0.49 m
First wall radius	0.6 m
Fusion power	2600 MW
Plasma power gain, Q	26
Average central beta	0.28
Peak central density	$3.3 \times 10^{20} \text{ m}^{-3}$
Ion temperature	24 keV
Electron temperature	24 keV
Central cell field	4.7 T
Peak choke coil field	24 T <sup>a</sup>
Yin-yang mirror field	7.5 T <sup>b</sup>
First wall loading	1.72 MW/m <sup>2</sup>
Anchor ICRH power, absorbed/ injected	5.7/6.7 MW each anchor
Plug neutral beam power, absorbed/injected	2.84/4.43 MW each plug
ECRH power, absorbed/injected	42/42 MW each plug
Copper coil and drift pumping power	50 MWe each end
Total recirculating power	~350 MWe <sup>c</sup>

Table I (continued)

---

Electric power from the direct converter	290
Total energy stored in magnets	49 GJ
<u>Efficiencies</u>	
Direct converter	0.51
475-kV sloshing ion beams	0.70
ECRH	0.70
Anchor ICRH	0.55

---

<sup>a</sup>16 T from outer superconducting coil plus 8T from copper insert coil.

<sup>b</sup>10 T on conductor.

<sup>c</sup>Includes recirculating power for coolant pumping and other plant functions.

because the decay afterheat is lower and the fissile fuel production per unit of thermal energy is higher than that of "fast-fission" blankets that utilize  $^{238}\text{U}$  or  $^{232}\text{Th}$  fissions induced by the 14.1 MeV neutrons to generate the excess neutrons for breeding. The lower afterheat leads to simpler, less risky, blanket designs, while the higher fuel production results in fewer fusion breeders and more attractive deployment scenarios. The reference fission-suppressed, fusion breeder can provide fissile makeup to fuel 13.5 LWRs of equal thermal power while a typical uranium fast-fission, fusion breeder can fuel fewer than 5 LWRs. (14,15)

## II. DESIGN OVERVIEW

### II.A. Design Description

After an extensive scoping phase<sup>(6,7)</sup> during 1981-1982 (see Section II.B), a reference blanket concept based upon flowing liquid lithium coolant radially through a two-zone packed bed of beryllium pebbles with thorium snap rings was selected. This concept, shown in Figure 1, has been designed in accordance with the specifications and performance levels provided in Table II.

The reference tandem mirror blanket design would be constructed from a low alloy ferritic steel (e.g., HT-9) and would be liquid lithium cooled. The blanket would operate at a moderate maximum temperature (425°C) and neutron wall loading (1.7 MW/m<sup>2</sup>). In terms of performance, technological development requirements and risk, this design can be classified as "moderate technology." For comparison, a "low technology" blanket could be developed using a low temperature (approximately 100°C) water-cooled design producing fuel but no power, while a "high technology" high performance blanket might be based upon helium cooling and Molten Salt Breeder Reactor technologies.<sup>(3)</sup>

The coolant flow in the blanket resembles that of a conventional oil filter. Specifically, coolant flows radially inward to the first wall plenum through a thin coolant annulus and is distributed to the packed bed through perforations in an intermediate wall which, in combination with the first wall and radial stiffening rings, provides a very stiff cylindrical structure. Having passed through the intermediate wall into the blanket, the coolant flows radially outward through two fuel zones (separated by another perforated wall), exits the bed through a third perforated wall outside of the second fuel zone, and exits the blanket through 20 large outlet pipes. The composite

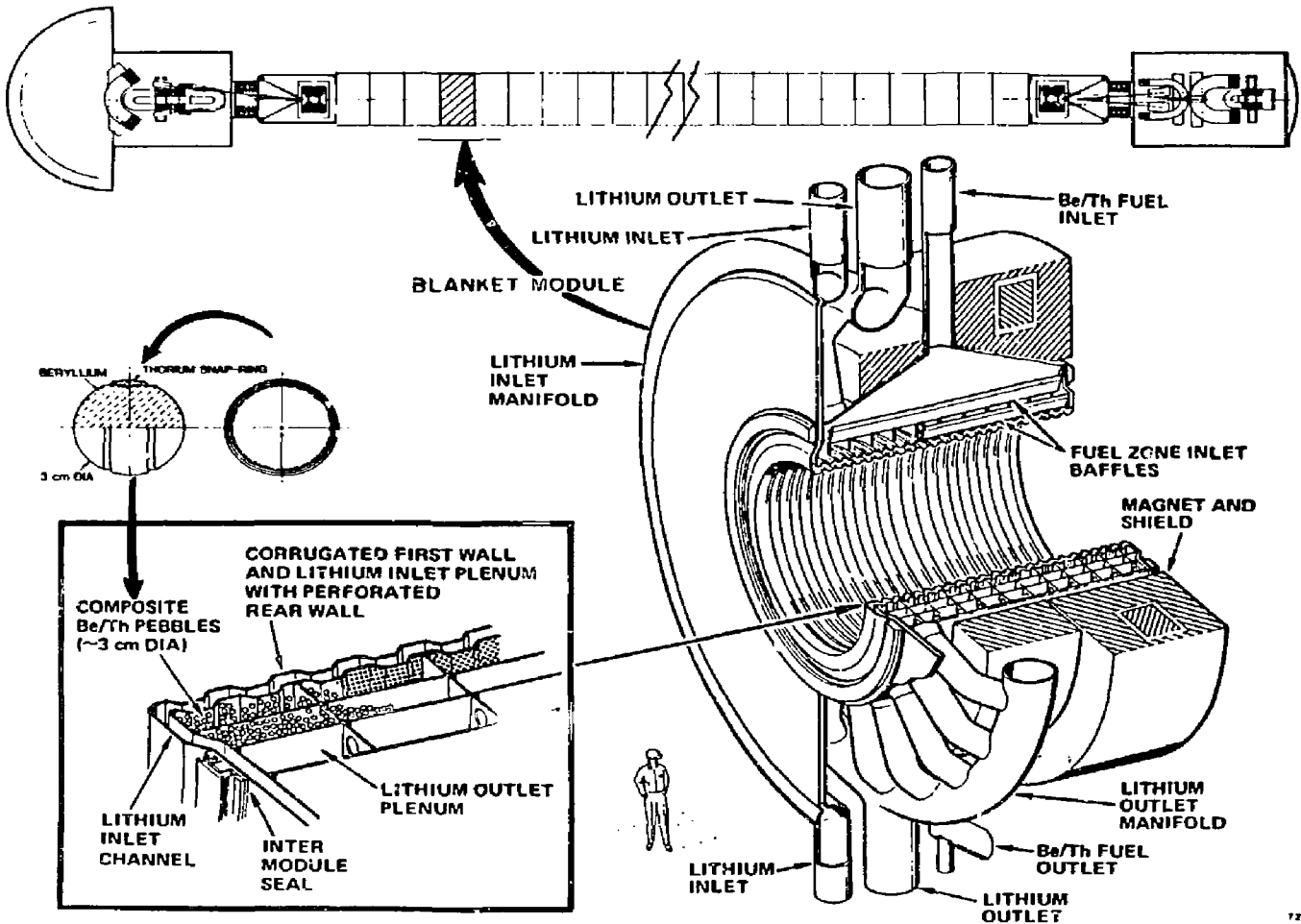


Figure 1.

The Reference Liquid Metal Cooled, Fission-Suppressed,  
Tandem Mirror Fusion Hybrid Blanket Features Direct  
Cooling of a Bed of Beryllium-Thorium Pebbles.

Table II.  
Key Design Specifications and Performance Parameters  
for the Reference Fusion Breeder Blanket

---

Global Parameters (70 percent capacity factor, average over system and time)

Central cell length	130 m
Number of blanket modules	32
Number of central cell coils	32
Central cell coil B field strength on axis	4.7
Central cell fusion power	2600 MW
Central cell fusion neutron power	2080 MW
Maximum central cell thermal power	5700 MW
Average central cell thermal power	5075 MW
$^{233}\text{U}$ fuel production	6656 kg/yr
Average in-core fissile inventory	5500 kg
Thorium throughput	630 MT/yr
Beryllium throughput	275 MT/yr

Blanket Module Mechanical Design

Structural material	HT-9 steel
Module length	4.1 m
Fraction of module length used for breeding $^{233}\text{U}$	~195%
First wall radius	1.5 m

---

Table II (continued)

Number of fuel zones	2
Fuel zone volume fractions:	
Beryllium (3.0 cm O.D. pebbles)	44%
Lithium	40%
Thorium (including bred fissile)	16%
Ferritic steel	2%
Thickness of each fuel zone	20 cm
Lithium reflector thickness	30 cm
Blanket outer radius	2.34 m
Shield thickness	75 cm
Magnet inner bore	6.7 m
Magnet pitch	4 m
Number of coolant outlet pipes	20 each

Heat Transfer, Power Flow, and Thermal Design Parameters  
(at maximum blanket M)

Neutron wall loading	1.72 MW/m <sup>2</sup>
Coolant	Lithium (3% <sup>6</sup> Li)
Maximum thermal power per blanket module	208 MW
Coolant inlet temperature	275°C
Coolant outlet temperature	425°C
Lithium flow rate per module	0.69 m <sup>3</sup> / sec
Lithium pressure drop	2.6 MPa (370 psi)
Maximum lithium pump power (per module)	1.8 MW

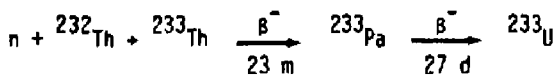
Table II (continued)

Maximum first wall pressure	1.7 MPa (225 psi)
Minimum first wall temperature	302°C
Maximum first wall temperature	353°C
Maximum structure temperature	425°C
Maximum beryllium surface temperature	410°C
Maximum beryllium internal temperature	445°C
Maximum beryllium $\Delta T$	~70°C
<u>Nuclear Design Parameters (at full power and 100 percent capacity factor)</u>	
Net fissile breeding ratio	0.84
Net tritium breeding ratio	1.06
Minimum blanket energy multiplication	1.71
Maximum blanket energy multiplication	3.17
Maximum thorium power density	70 W/cm <sup>3</sup>
Maximum beryllium power density	9.1 W/cm <sup>3</sup>
Maximum lithium power density	4.5 W/cm <sup>3</sup>
Zone 1 fuel residence time	316 full power days
Zone 2 fuel residence time	532 full power days
Average uranium discharge concentration	1.00%
Average protactinium discharge concentration	0.05%
Average fission rate per fusion	0.09
Average fission burnup at fuel discharge	~1000 MWD/MTHM

fuel pebbles (3 cm O.D. beryllium pebbles with thorium snap-rings) are loaded into the top of the blanket and discharged at the bottom in a batch process.

The breeding performance is excellent for two reasons. First, the design features a high volume fraction of high efficiency neutron multipliers. The bed volume fractions in Figure 1 include 44 percent beryllium, 40 percent lithium, and 16 percent thorium - all excellent neutron multipliers.<sup>a</sup> The remainder of the fuel zones following the wall is less than 2 percent steel. Second, the design effectively suppresses the fissioning in the blanket. Fast fissioning is suppressed due to neutron moderation in the beryllium and the low thorium volume fraction. Thermal and epithermal fissions in the bred <sup>233</sup>U are suppressed due to both fuel discharge at low fissile concentration (<1 percent <sup>233</sup>U in the small volume of thorium) and thermal neutron depletion (due to the large 1/v neutron absorption cross section of <sup>6</sup>Li).

As a result, fission product inventories and decay afterheat levels in the fuel are very low. In fact, as shown in Figure 2, the fission product decay afterheat is a relatively minor contribution to the total afterheat. Rather, the afterheat associated with actinide decay through the chain



dominates the overall afterheat level. Typical fission product levels in the discharge fuel are only about 1000 ppm in thorium, or roughly one-thirtieth that of LWR discharge fuel. The reduced fission product afterheat is uniquely associated with fission-suppressed blankets since fast-fission blankets, with

---

a) Lithium is not, in a strict sense, a neutron multiplier. However, its <sup>7</sup>Li (n,n' $\alpha$ )<sup>3</sup>H reaction results in tritium breeding without the loss of a neutron.

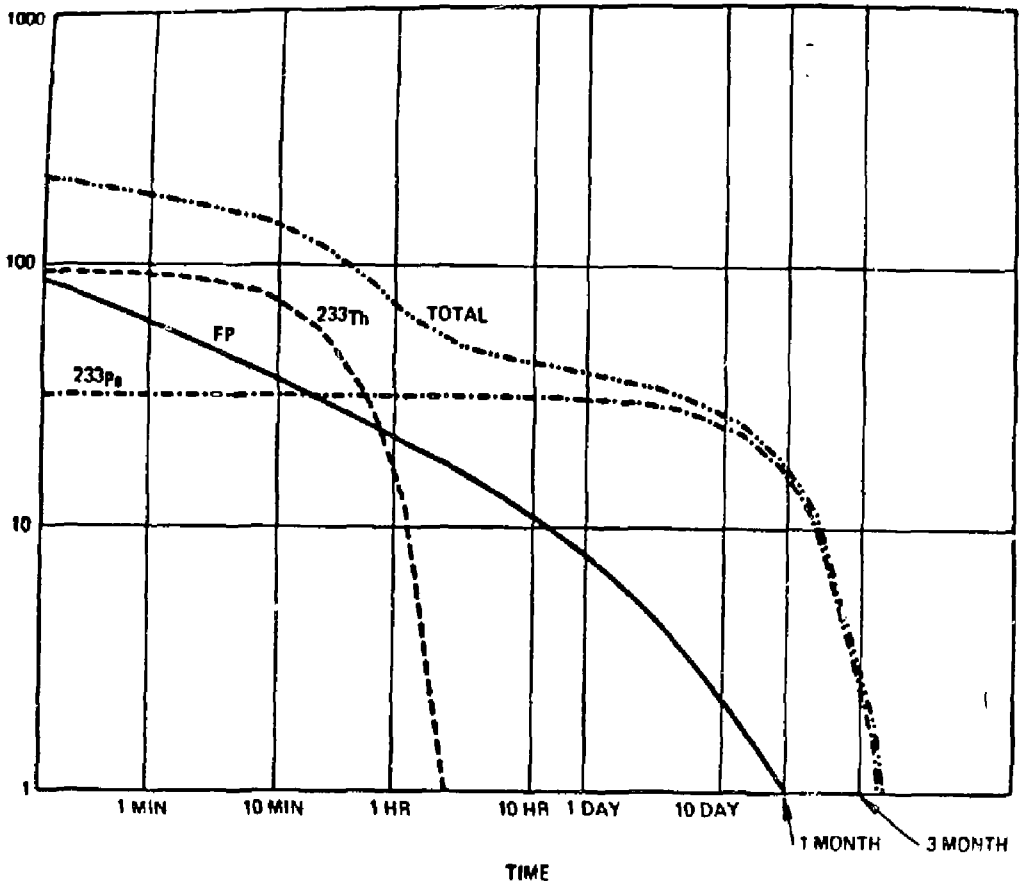


Figure 2.  
Relative Contributions to the Afterheat in Suppressed  
Fission Blankets

blanket energy multiplications of about 10, increase the fission rate by an order of magnitude.

The use of a mobile fuel form (i.e., the composite beryllium/thorium pebbles), with provision to discharge the fuel to an independently cooled dump tank should the need arise, results in important reactor safety benefits. In addition to the primary coolant loop, the dump tank/fuel handling system piping and valving, shown schematically in Figure 3, provide a coolant flow sufficient to remove the decay afterheat. Therefore, double redundancy of the internal cooling systems can be provided. Independent shield and first wall cooling systems can also cool the blanket internals from the exterior surfaces, providing a third level of redundancy.

The composite beryllium/thorium pebble fuel form provides several additional advantages. The beryllium and thorium can be uniformly mixed throughout the blanket - an advantage with respect to the nuclear breeding performance. Also, the design is relatively insensitive to low levels of volumetric swelling in the beryllium, since it can be circulated periodically and the packing density of the bed, although high, is low enough to accommodate some growth (typically 0.1 percent linear growth occurs over the 0.9 full power year irradiation cycle). Finally, the small size of the pebbles (1.5 cm radius) limits the thermal and differential swelling induced stress levels in the beryllium - key lifetime determinates. Our results indicate that an average beryllium in-core lifetime in excess of three years should be achievable, but that more materials data and more accurate models are required before a definitive lifetime estimate will be possible. (5,9)

## II.B. Blanket Materials Selection

Several key choices of materials and operating limits were made early in

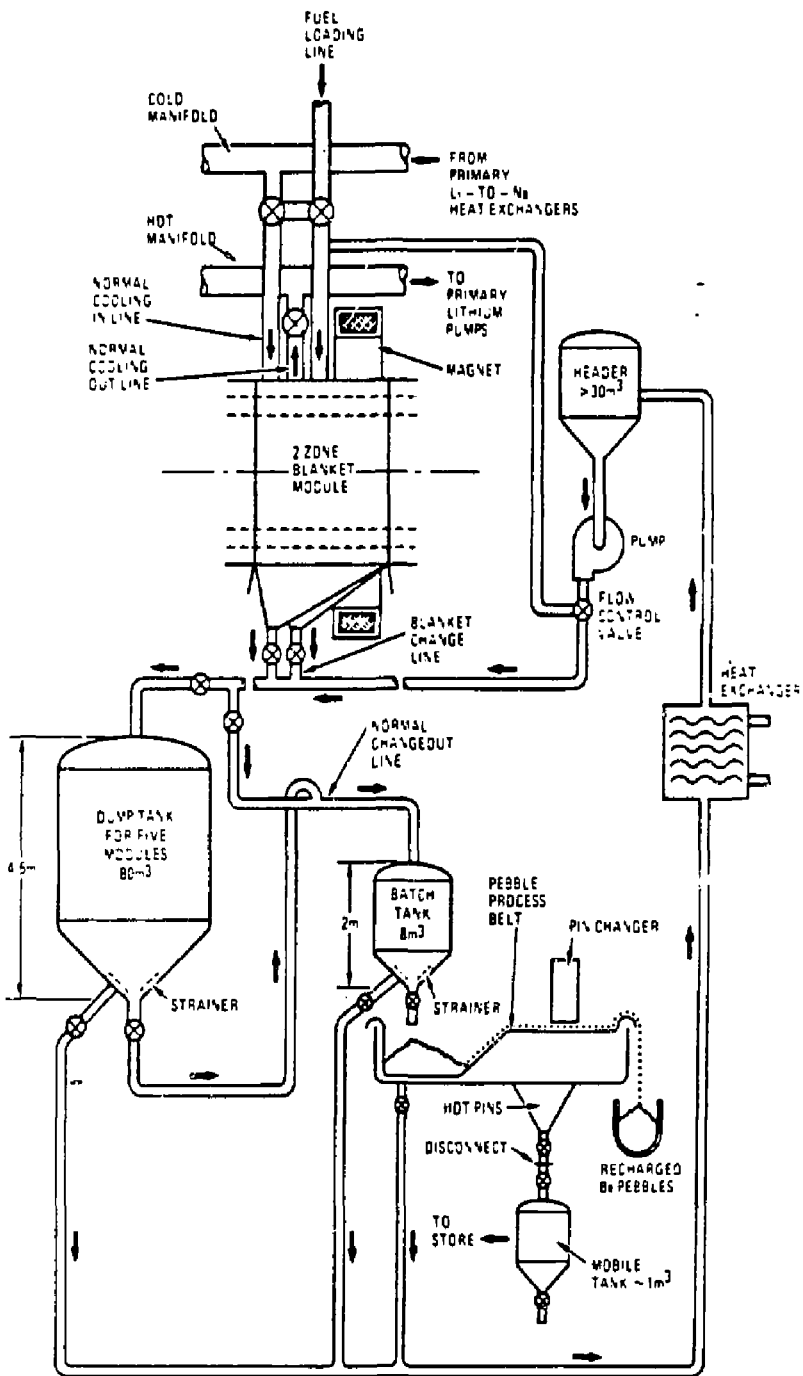


Figure 3.

Schematic Diagram of Fusion Breeder Fuel Handling Circuit.

the study. These included the choice of a structural material and neutron fluence limit and the choice of a primary coolant and operating temperature limit.

For structural support, both ferritic steels [e.g., 12 Cr-1 Mo (HT-9) or 2-1/4 Cr-1 Mo] and austenitic steels [e.g., titanium modified 316-stainless steel (PCA)] were considered. As shown in Table III,<sup>(16)</sup> ferritic steels provide several advantages:

- lower swelling
- lower thermal stress
- lower irradiation creep
- lower corrosion in liquid metals

Most importantly, assuming a displacement damage accumulation rate of 15 dpa/MW-yr, a 190 dpa radiation lifetime implies a maximum blanket life for the reference fusion breeder blanket of 10.6 calendar years. Even if a full year is required to replace blanket assemblies at end-of-life (much longer than previous estimates),<sup>(10,11)</sup> the impact upon average plant capacity could still be less than 10 percent.

In comparison, recent fusion-electric reactor and blanket studies<sup>(12,13,16)</sup> postulate much higher neutron wall loads (approximately 5 MW/m<sup>2</sup>) to achieve compact fusion reactor cores. Requirements for high allowable fluences and/or quick blanket replacement will be increased several-fold in comparison with the fusion breeder.

The key issues associated with the choice of a ferritic steel structure are as follows:

- elevation of the ductile-to-brittle transition temperature (DBTT) above room temperature
- a requirement for post-weld heat treatment to re-establish mechanical properties

Table III.  
Summary of Structural Materials Assessment  
(from Reference 16)

Austenitic Steel Candidate Alloys	Ferritic Steel PCA-CW	Vanadium HT-9	V-15 Cr - 5 Ti
Thermal stress factor $MW/m^2-mm$ ( $500^\circ C$ )	3.2	4.8	9.8
Maximum surface heat flux, $MW/m^2a$	0.3	0.4	1.8
Design stress limit  $S_{gt}$ (MPa) ( $2 \times 10^4$ , 100 dpa, $550^\circ C$ )	100	155	165
Maximum allowable temperature, $^\circ C$ ( $\sim 0.5 T_m$ ) (irradi- ation embrittlement)	550	550	720
Lithium Corrosion rate at $500^\circ C$ , $mg/m^2 \cdot h^b$	60	2	$< 0.01$
Radiation lifetime (swelling) (5%)	100 DPA ( $500^\circ C$ )	190 DPA <sup>d</sup>	220 DPA <sup>c</sup>
Critical design issues <ul style="list-style-type: none"> <li>• High thermal stress</li> <li>• Liquid metal corrosion</li> <li>• Radiation creep</li> <li>• Operating temper- ature limit</li> </ul>	<ul style="list-style-type: none"> <li>• Limited lifetime (swelling)</li> <li>• DBTT above RT</li> <li>• Operating temperature limit</li> <li>• Liquid metal embrittlement</li> <li>• Ferromagnetic Properties</li> </ul>	<ul style="list-style-type: none"> <li>• Weld procedure (PWHT)</li> <li>• Weld procedure (inert environment)</li> <li>• Oxidation characteristics</li> <li>High T permea- iation rates</li> <li>• Costs</li> </ul>	<ul style="list-style-type: none"> <li>• R&amp;D requirements</li> </ul>

<sup>a</sup>Idealized flat plate 5 mm thick with  $50^\circ C$  film coefficient,  $T_{out} = 400^\circ C$ .

<sup>b</sup>Predicted for 1.5 m/s.

<sup>c</sup>Not well defined, may be higher.

- increased loads due to the ferromagnetic properties of the alloy

Regarding the first issue, it is important that the DBTT be maintained at less than the blanket operating temperature. This requires that the minimum operating temperature for irradiated structure be above 290°C and that the minimum coolant temperature in the reference design be greater than 275°C. Although the operating DBTT will in this case be above room temperature, experimental results indicate that prior to normal shutdown, the blanket structure can be annealed at approximately 450°C for approximately 40 hours such that the DBTT will be returned to below room temperature. (2,17) Typical calculations of the change in DBTT and the expected effects of annealing are shown in Figures 4a and 4b. The increase in wall load from 1.3 MW/m<sup>2</sup> (shown in the figure) to 1.7 MW/m<sup>2</sup> is not expected to change these results in a qualitative sense.

The choice of liquid lithium as the blanket coolant derives from several advantages. Lithium has been shown to be less corrosive than Pb-Li Li<sub>17</sub>Pb<sub>83</sub> in the 400 to 500°C operating range (16) and its use is less likely to result in heat exchanger tube plugging or other damaging mass transfer mechanisms. Lithium also has a much higher tritium solubility than Pb-Li so that normal tritium releases will be very low while allowing for efficient tritium extraction. (18,19) Finally, lithium is lighter than the beryllium-thorium fuel pebbles while Pb-Li is heavier. This is an important consideration for fusion breeder blanket fuel management and safety because the gravity dump feature anticipates that the heavier fuel will not become uncovered during discharge.

Although the potential for radioactivity releases via the strong reaction between lithium and water is a clear concern, it is our considered opinion that liquid lithium systems can be designed to operate more reliably than

lead-lithium systems and will have the advantage of lower normal tritium releases. An acceptable level of lithium safety appears to be achievable based upon the development of liquid sodium coolant safety systems in the LMFBR program.<sup>(2,5)</sup> A recognition that fusion breeder reactors would not, most likely, be sited near population centers (but, rather, in remote safeguarded fuel cycle centers) provides additional motivation for the choice of a liquid lithium coolant.

The choice of thorium metal as a fertile fuel form rather than thorium dioxide (thoria) or another thorium form is primarily based upon fuel cycle considerations. Specifically, thorium metal is less expensive to reprocess using conventional aqueous or advanced pyrochemical techniques.<sup>(2,20)</sup> There is, however, a concern regarding the potential for solid-solid chemical reactions (Th-Be, Th-Th self welding) and/or fission product release in the liquid metal bath.<sup>(2,5)</sup> If these effects are substantial, then the use of a thin coating (Mo, ThO<sub>2</sub>, ThC, or TiC) should be investigated.

Similarly, there is a concern relative to Be-Be self-welding which might result in pebble sticking. In this case the use of a thin beryllium coating (Be<sub>12</sub>Fe, Be<sub>12</sub>Cr, Be<sub>12</sub>Mo) can be investigated as a means of mitigating both Be and Be-Th interactions. Although some experimental work has been conducted to determine the extent of chemical interactions for the reference fusion breeder blanket,<sup>(2)</sup> more work in this area is needed. Our choice of 425°C as the maximum blanket temperature should be conservative with respect to materials compatibility issues.

Finally, it should be noted that the use of a vanadium alloy in the fusion breeder blanket would allow higher operating temperatures, providing benefits in several areas (lower pressure drops, higher thermal efficiency, higher safety margin). This more advanced option has not been considered in detail, but its application to the fusion breeder is clearly no more difficult than its application to the self-cooled lithium/vanadium fusion-electric blankets for which it has been proposed.<sup>(16)</sup>

### III. KEY DESIGN AREAS

Several features of the reference fusion breeder design are discussed in more detail in this section. Each of these was addressed as a "special topic" during 1983-1984<sup>(5,8,9)</sup> after the initial design concept was developed during 1982.<sup>(2)</sup> The intent of this section is to introduce the reader to the unique design and analysis issues associated with the reference fusion breeder blanket described in the previous Section.

#### III.A. Nuclear Design and Fuel Management

The economic attractiveness of the fusion breeder is strongly dependent upon its ability to supply excess neutrons for fissile breeding above and beyond the requirement for tritium self-sufficiency. Consequently, the nuclear performance of the reference fusion breeder blanket continues to be a primary focus in design studies.

Beryllium, the principal constituent in the reference blanket, is a very strong neutron energy moderating material. Consequently, local heterogeneities and resonance self-shielding in the thorium have been recognized as being very important to the development of a realistic estimate of the net breeding performance. Tacnikowski<sup>(21)</sup> was the first to point out that the fusion breeder blanket, as originally defined in 1982 [55 volume percent Be, 3 % Th (including bred  $^{233}\text{U}$ ), 40 % Li (0.2 a/o  $^6\text{Li}$ )] would produce substantially more tritium, less  $^{233}\text{U}$  and more energy than had been expected prior to consideration of resonance self-shielding effects. Later, it was shown<sup>(5,22,23)</sup> that by increasing the thorium volume fraction in the bed, it would be possible to both increase fissile production relative to tritium

production and lower the energy multiplication of the blanket.

The calculational method used to select the optimal thorium volume fraction and estimate the breeding performance of the reference breeder involves the use of a 1-D ANISN<sup>(24)</sup> blanket model with a LANL version of ENDF/B-IV and V cross sections<sup>(25)</sup> which were adjusted to account for resonance self-shielding and spatial self-shielding effects. The 1-D results were then adjusted to account for multidimensional effects (e.g., the sides of each blanket module) by comparison with previous 2-D TARTNP Monte Carlo models of the reference blanket.<sup>(2)</sup>

The 1-D results were also compared with the results of a 1-D Monte Carlo analysis using the LLNL ALICE Code<sup>(26)</sup> and ENDL nuclear data.<sup>(27)</sup> The beryllium cross section data in ENDL has been compared with recent experimental data at LLNL<sup>(8)</sup> and was found to be adequate for design purposes.

The resulting nuclear performance is shown in Figure 5, where the net fissile production (including losses due to in-situ fissioning) and energy multiplication are estimated as a function of the thorium concentration in the blanket.<sup>(5)</sup> The results indicate that by increasing the thorium concentration from 3 percent to 16 percent, the net fissile production will nearly double, while the maximum blanket energy multiplication,  $M$ , will decrease significantly. Beyond approximately 16 percent, the fissile production ceases to increase and the energy begins to rise as  $^{232}\text{Th}$  (n,f) reactions become more important.

As shown in the figure, and in Table IV (where the beginning-of-cycle, end-of-cycle, and average performance are shown), a 1 percent  $^{233}\text{U}$  average discharge enrichment,  $\epsilon_d$ , has been selected for the reference blanket. The optimal discharge enrichment is a function of the fissile recovery cost (which favors a high  $\epsilon_d$ ), the carrying cost for maintaining an inventory of fissile material in the blanket (which favors a low  $\epsilon_d$ ) and other factors such as

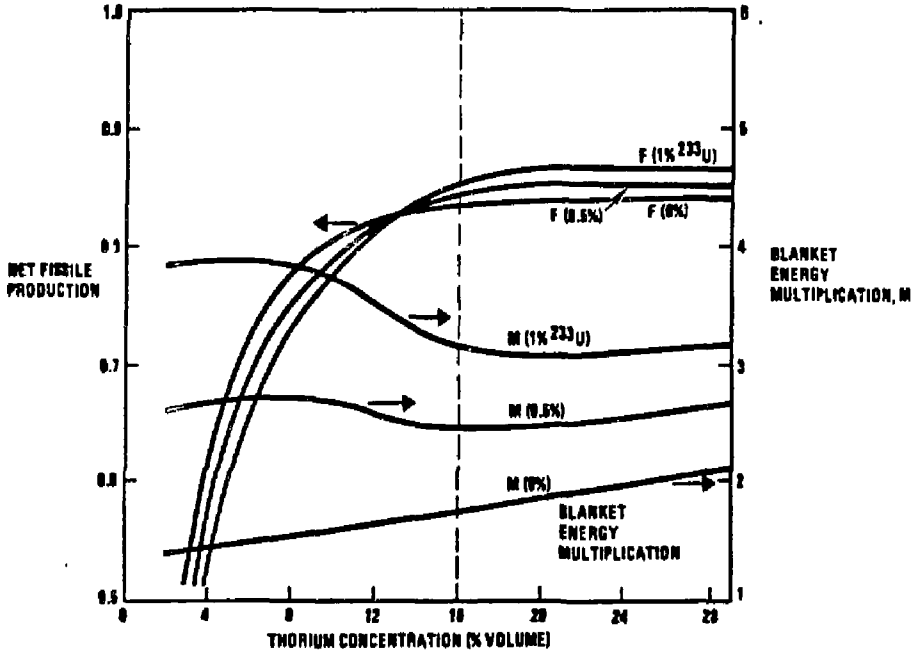


Figure 5.

Net Fissile Production and Blanket Energy Multiplication  
 versus Thorium Concentration for Fixed Tritium  
 Breeding ( $T = 1.06$ )

Table IV.  
Nuclear Performance for 16 Percent Thorium and  
1 Percent  $^{233}\text{U}$  Average Discharge Enrichment

	BOC	EOC <sup>a</sup>	Average
Net fissile breeding per fusion	0.834	0.853	0.844
Blanket energy multiplication <sup>b</sup>	1.71	3.17	2.44
Tritium breeding	1.06	1.06	1.06
Ideal $^6\text{Li}$ enrichment (%)	3.4	2.6	3.0
Thorium fissions	0.033	0.035	0.034
Uranium fissions	0	0.107	0.053

<sup>a</sup>1 percent  $^{233}\text{U}$  plus 0.05 percent  $^{233}\text{Pa}$  in thorium.

<sup>b</sup>blanket energy per fusion divided by 14.1 MeV

criticality and the effects of an increased blanket power swing over the fuel residence time. In general,  $\epsilon_d$  values in the range 0.5 to 1.0 have been considered for fusion breeder blankets with hatch fueling. The lower value is most appropriate when inexpensive fissile recovery techniques, such as pyrochemical reprocessing<sup>(20)</sup> are available.

The blanket energy multiplication,  $M$ , for each individual blanket module varies between 1.71 and 3.17 over a fuel residence period which is split into two halves. Specifically, fuel would be removed from the inner breeding after each 45 full power week irradiation period. After the first half cycle, the blanket  $M$  will increase to approximately 2.9. A fresh load of fuel would then be placed into the inner zone such that it and the outer zone would be irradiated for an additional 45 week period prior to the discharge of fuel from both zones. Immediately prior to discharge, the maximum blanket  $M$  of 3.17 would occur.

The large power swing indicated above is not desirable for the fusion breeder as a whole because, for a fixed fusion power, it results in an under-utilized thermal power conversion system (at BOC) as well as the institutional difficulties associated with producing different levels of electricity at different points in the cycle. Fortunately, this problem can be greatly reduced if the 32 blanket modules of the central cell are divided into four groups of differing fuel zone maturity (but identical design). In this case, shown in Figure 6, if three-eighths of the fuel is discharged each 22.5 full power week (i.e., at quarter-intervals of the full fuel residence period). By staggering the fuel zone maturity in this way, the system power swing can be limited to the range of  $M$  values between 2.14 and 2.74. Taking 2.44 as the average value, the resulting power swing is only  $\pm 12$  percent (rather than  $\pm 30$  percent for an individual blanket).

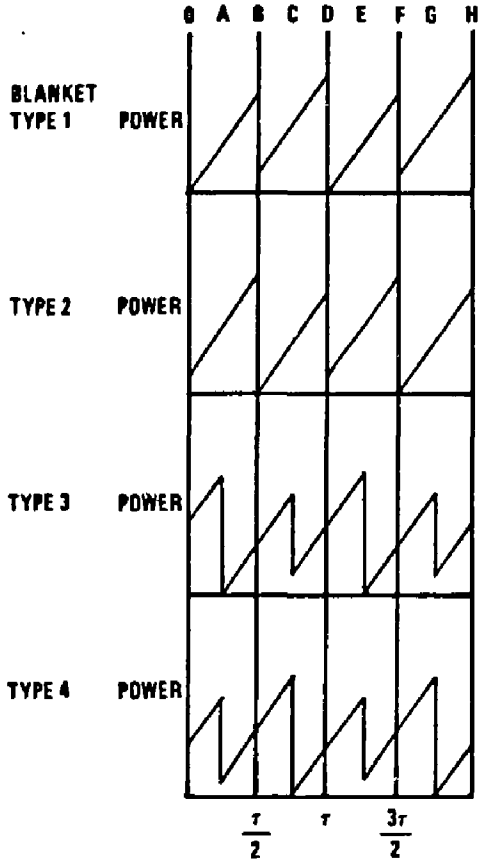


Figure 6.

The Blanket Power Swing Would be Minimized by Dividing  
the 32 Module Central Cell into Four Groups  
of Differing Fuel Zone Maturity

An overall fuel management cycle, reflecting the above strategy for minimizing the power swing, and achieving an average plant availability factor of 70 percent, is shown in Table V. This cycle would include a 1 week down time allocation between each 22.5 full power week (26.5 calendar week) cycle to allow for fuel changeout and scheduled maintenance. After four such cycles (25.4 months) an extended down time allocation of 18.6 weeks (4.3 months) is provided for major maintenance including changeout of 8 of the 32 blanket modules. Thus the replacement irradiation dose for a blanket module would be  $4 \times 4 \times 22.5 = 360$  full power weeks at  $1.72 \text{ MW/m}^2$ , or  $11.9 \text{ MW-yr/m}^2$ . Assuming a structural damage rate of 15 dpa per  $\text{MW-yr/m}^2$ , the replacement damage is below the 190 dpa limit discussed earlier.

### III.B. Liquid Metal Coolant Flow

Magnetohydrodynamic (MHD) effects which result from the use of liquid metal coolants include the modification of flow profiles (including the suppression of turbulence) and increases in the primary loop pressure drop and the hydrostatic pressure at the first wall of the blanket. In the reference fission-suppressed tandem mirror fusion breeder design concept, the surface heat flux is very low and heat transfer limitations due to flow profile modification are a relatively minor concern, but the required first wall structure thickness is directly related to the MHD pressure drop in flowing the liquid lithium coolant. As such, it is a major concern which directly impacts fissile breeding efficiency.

One equation that blanket designers can use with confidence to calculate liquid metal MHD pressure drops is for Hartmann flow in a simple circular or rectangular channel. However, large uncertainties still exist for the following, more complicated, flow configurations which occur in the reference fusion breeder blanket:

Table V. Fusion Breeder Operational Cycle This cycle would repeat every 1.85 calendar years  
(representing three-quarters of a full period).

	Operation	Fuel Change	Operation	Fuel Change	Operation	Fuel Change	Blanket Change (8 modules)	Operation	Fuel Change
Duration (CY)	0.51	0.02	0.51	0.02	0.51	0.02	0.36	0.51	0.02
Duration (calendar weeks)	26.5	1	26.5	1	26.5	1	18.6	26.5	1
Capacity factor (%)	85	0	85	0	85	0	0	85	0
Equivalent number of full power weeks	22.5	0	22.5	0	22.5	0	0	22.5	0

- Flow through a packed pebble bed.
- Flow through bends (for both legs perpendicular to the B-field and one leg perpendicular).
- Flow through a B-field gradient.
- Flow through channels with varying conducting wall thickness.
- Flow at an angle to the magnetic field.
- Flow through contractions, expansions, and distribution plena.
- Flow through ducts which incorporate electrically insulating materials.

Although we are reasonably confident regarding the ability to flow liquid metals in this design (i.e., the magnetic field of 4.7 T and neutron wall load of  $1.72 \text{ MW/m}^2$  are low compared with those expected in a tokamak), it is clear that an experimental confirmation of pressure drop scaling in the relevant flow regime will be required.

### III.B.1 Packed Bed Pressure Drop

Because the packed bed flow is unique to this design, an improved model for the packed bed pressure drop has been developed.<sup>(5)</sup> By considering spatial averages of the electric fields, currents, and fluid flow velocities, the general electro-hydrodynamic equations have been reduced to simple expressions for the pressure drop. These expressions involve a constant which reflects unknown details of the flow around the pebbles, but an energy approach has been used to attempt to bound the possible values of the constant, and thus the pressure drop.

The geometry of interest is shown in Figure 7. A liquid metal coolant flows radially outward from the inner surface at  $R_0$  ( $= 1.59 \text{ m}$ ) to the outer surface at  $R_1$  ( $= 1.99 \text{ m}$ ). The unperturbed magnetic field  $B_0$  ( $= 4.7 \text{ T}$ ) is

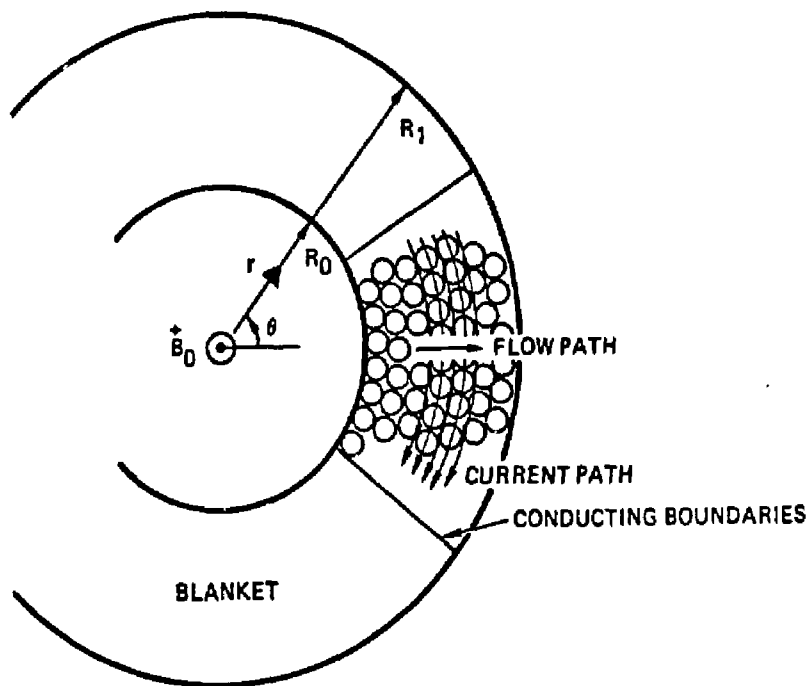


Figure 7.  
 The Coordinates, Geometry, and Current Paths  
 in the Reference Blanket.

assumed to be uniform, and is oriented along the Z axis of the cylinder. The blanket is assumed to be segmented by perfectly conducting radial boundaries. With this boundary condition the average azimuthal electric field is zero in the blanket. This is equivalent to having no radial boundaries at all.

The nonlinear differential equations of electro-hydrodynamics result in a simple linear differential equation for the pressure drop if:

- the flow is laminar,
- variations in the magnetic field are negligible on the scale length of a pebble,
- inertial forces are small compared to the magnetic force,
- viscous forces are small compared to the magnetic force.

These criteria are satisfied in the reference blanket because the Reynolds number,  $Re$ , the magnetic Reynolds number,  $Rm$ , the Hartmann number,  $H$ , and the magnetic interaction number,  $N$ , satisfy the following criteria:

$$Re = d \langle U \rangle \frac{\rho}{\eta} < 5 \times 10^5 B_0 \quad (1)$$

$$Rm = \sigma \langle U \rangle \mu d \ll 1, \quad (2)$$

$$H = \kappa B_0 \left( \frac{\sigma}{\eta} \right)^{1/2} \gg 1, \quad (3)$$

$$N = \sigma B_0^2 \frac{d}{\rho \langle U \rangle} \gg 1, \quad (4)$$

where  $d$  is the pebble diameter (3 cm),  $\langle U \rangle$  is the average coolant speed (= 4.5 cm/s at the inner radius), and  $\rho$ ,  $\eta$ ,  $\sigma$ ,  $\mu$  are the coolant density, the absolute viscosity, electrical conductivity, and the magnetic permeability

(given by  $486 \text{ kg/m}^3$ ,  $3.8 \cdot 10^{-4} \text{ kg/m/s}$ ,  $3.2 \cdot 10^6 \text{ mho/m}$ , and  $4\pi \cdot 10^{-7} \text{ H/m}$ , respectively). The numerical constant on the right hand side of Eq. (1) was suggested by Hoffman and Carlson for flows with  $H < 2000$  and  $B_0$  given in Tesla. (28) The average radial speed  $\langle U \rangle$  of the coolant in the pebble bed blanket is inversely proportional to the pebble bed void fraction  $\epsilon$ . The void fraction has a theoretical minimum of 0.25 for spherical pebbles, but for random packing a more likely value is 0.4.

The above criteria being satisfied, the momentum and field equations reduce to

$$\Delta P = \vec{j}_f \times \vec{R} \quad (5)$$

and

$$\Delta \times \vec{R} = \mu \vec{j} \quad (6)$$

where  $P$  is the pressure in the fluid,  $J$  is the current density, and the subscript  $f$  denotes fluid quantities. Averaged over the blanket, the pressure gradient is radial and the currents in the fluid and pebbles are azimuthal. The average azimuthal current in the fluid follows from Ohm's law:

$$\langle J \rangle_f = \sigma_f \langle U \rangle B (K-1), \quad (7)$$

where  $K$  is defined as the ratio of the average electric field in the fluid divided by  $\langle U \rangle B$ . The quantity  $K$  is an intrinsic property of only the pebble-to-fluid conductivity ratio, the volume fraction  $\epsilon$ , and the boundary conditions on either the average azimuthal current or electric field. This

constant can be evaluated precisely if the local flow field can be precisely described. However, because of the complex nature of the local flow field, it will suffice to point out that K is between zero and unity.

The magnetic induction, B, follows from an integration of Ampere's law. Before the integration can take place, the boundary condition on the azimuthal electric field  $\langle E \rangle$  averaged over the blanket must be specified. The boundary condition of  $\langle E \rangle = 0$  leads to

$$B(r) = B_0 \left(\frac{r}{R_0}\right)^{Rm[1 + K(S-1)]} \quad (8)$$

where S is the conductivity of the pebbles divided by that of the fluid.

Having specified the average azimuthal current in the fluid and the magnetic induction B, the momentum equation can be integrated for the average pressure drop across the blanket:

$$\langle \Delta P \rangle = \sigma_f \langle U_0 \rangle B_0^2 R_0 (1-K) \frac{(R_1/R_0)^{2Rm[1+K(S-1)]} - 1}{2Rm[1+K(S-1)]} \quad (9)$$

The only quantity not yet precisely defined is the intrinsic constant K. So far it has only been stated that K is between zero and unity. As part of this analysis the energy equation was used to reduce the uncertainty in K. It was found that

$$0 < K < 1 / (1 + \frac{S_E}{1-E}) \quad (10)$$

Eq. (10) can be used to show the exponent in Eq. (9) is much less than unity, even if  $S \rightarrow \infty$ . Thus, Eq. (9) reduces to

$$\langle \Delta P \rangle = \sigma \langle U_0 \rangle B_0^2 R_0 (1-k) \ln(R_1/R_0) \quad (11)$$

As a practical application of the above analysis, consider the reference blanket. For beryllium pebbles and lithium coolant  $S = 2$ . From Eqs. (10) and (11)

$$1.2 \text{ MPa} > \langle \Delta P \rangle > 0.6 \text{ MPa}$$

### II.B.2 Pressure Drop Summary

Pressure drop estimates for MHD flow over the entire blanket circuit are shown in Table VI. The estimates for flow outside of the packed bed are based upon the various pressure drop terms described in References 2 and 28.

A particular concern is the outlet plenum, where an insulated pipe<sup>(6,16)</sup> with an effective wall thickness of 1 mm is assumed. Although the simple, cylindrical geometry of the plenum should be amenable to the development of such a component, insulated piping concepts capable of surviving cyclic thermal and pressure loadings in a high radiation field could prove to be difficult. Interestingly, the inlet plenum pressure drop is not a significant concern because it does not affect the first wall pressure, the key determinate of the overall hydrostatic loading of the blanket.

The estimated first wall pressure of 1.6 MPa (232 psi) can be accommodated by the blanket structural support without an excessive neutronic penalty. The overall pressure drop of 2.6 MPa (377 psi) results in a peak pumping power of 1.8 MW per module at end-of-life (highest blanket energy multiplication). On average, less than 1 percent of the overall thermal power would be consumed as liquid metal pump power.

Table VI.  
Summary of Overall MHD Pressure Drop Estimate

	Pa
Inlet plenum <sup>a</sup>	$7.3 \cdot 10^5$
First wall	$1.1 \cdot 10^3$
Packed bed	$1.2 \cdot 10^6$
Lithium reflector	$3.4 \cdot 10^4$
Outlet plenum and pipes <sup>a</sup>	$1.1 \cdot 10^5$
Turns, contractions, expansions <sup>b</sup>	$5.9 \cdot 10^5$
Total	$2.6 \cdot 10^6$
First wall pressure	$1.6 \cdot 10^6$
Pumping power (peak)	1.8 MW/mod.
Pump/thermal power <sup>c</sup>	0.9%
Average pump/thermal power <sup>d</sup>	0.7%

<sup>a</sup>Insulated pipe - 1 mm thick wall assumed.

<sup>b</sup>Assumed pressure drop coefficient  $K = 0.06$  (see Reference 2 discussion).

<sup>c</sup>At peak power.

<sup>d</sup>Over entire plant.

### III.C.1 Structural Design Requirements and Design Features

In this section, the structural design approach is discussed, the results of an axisymmetric structural model used to estimate thermal and pressure stresses in an earlier version of the reference blanket are presented, and design improvements are suggested. These topics are described in more detail in References 2 and 5.

The ferritic steel (HT-9) blanket structure is required to provide normal and transient stress levels which lead to an acceptable blanket lifetime of at least 4 to 5 full power years. At the same time, the design must provide a first wall (and intermediate wall) structure which is thin enough so that breeding performance in the blanket is maximized. Thirdly, the design must provide internal structure to serve as a zone separator and conduit for the mobile fuel.

The structural loading of the reference blanket results from the sum of three contributions:

- The MHD flow induced coolant pressure loading.
- Thermally induced loads due to the radial variations in the coolant temperature (i.e., the hotter back wall expands more than the cooler first wall).
- Dead weight gravity loads.

In response to these loads, the blanket will deform elastically (and possibly plastically in localized areas), and will undergo volumetric swelling and irradiation creep, which will determine the structural lifetime.

In order to increase stiffness and withstand the compressive buckling pressure due to the coolant, the first wall is connected to a thicker intermediate wall which separates the first wall coolant annulus from the

fertile fueled region. The connections between these two walls consist of 90 radial ribs equally spaced around the first wall/intermediate wall assembly and extending the full length of the module (see Figure 8). By corrugating the first wall circumferentially, the first wall thickness of 0.36 cm is capable of withstanding the bending stresses. The 0.64 cm perforated intermediate wall is also corrugated to increase the stiffness. A feature of the original design, shown in Figure 9, is the connection of the double shell first wall/intermediate wall assembly to the thick outer wall of the module via several radial support plates. These plates extend from the intermediate wall, through the fuel zone separators and outer lithium plenum, to the outer wall of the module. The (~1/cm) radial support plates are similar to tubesheets in a heat exchanger. The plates are spaced axially at approximately 30 cm intervals to provide additional radial support to sustain the coolant pressure compressive load on the first wall/intermediate wall assembly. The spacing between radial supports is consistent with maintaining adequate space for the fuel pebbles to flow freely. As indicated in Figure 10, additional structure is required at the top and bottom of the blanket to guide the pebbles into the blanket and out of the individual fuel zones.

### III.C.2 Stress Modeling

As mentioned above, an axisymmetric elastic stress model was used to estimate the steady state stress levels in the original (1982) version of the reference blanket. The model, consisting of plate and shell elements, is shown in Figure 11. It should be noted that the left hand side of the model is located at the axial midpoint of the blanket (symmetry condition) and that the right hand side represents the end of the module. As shown, some details

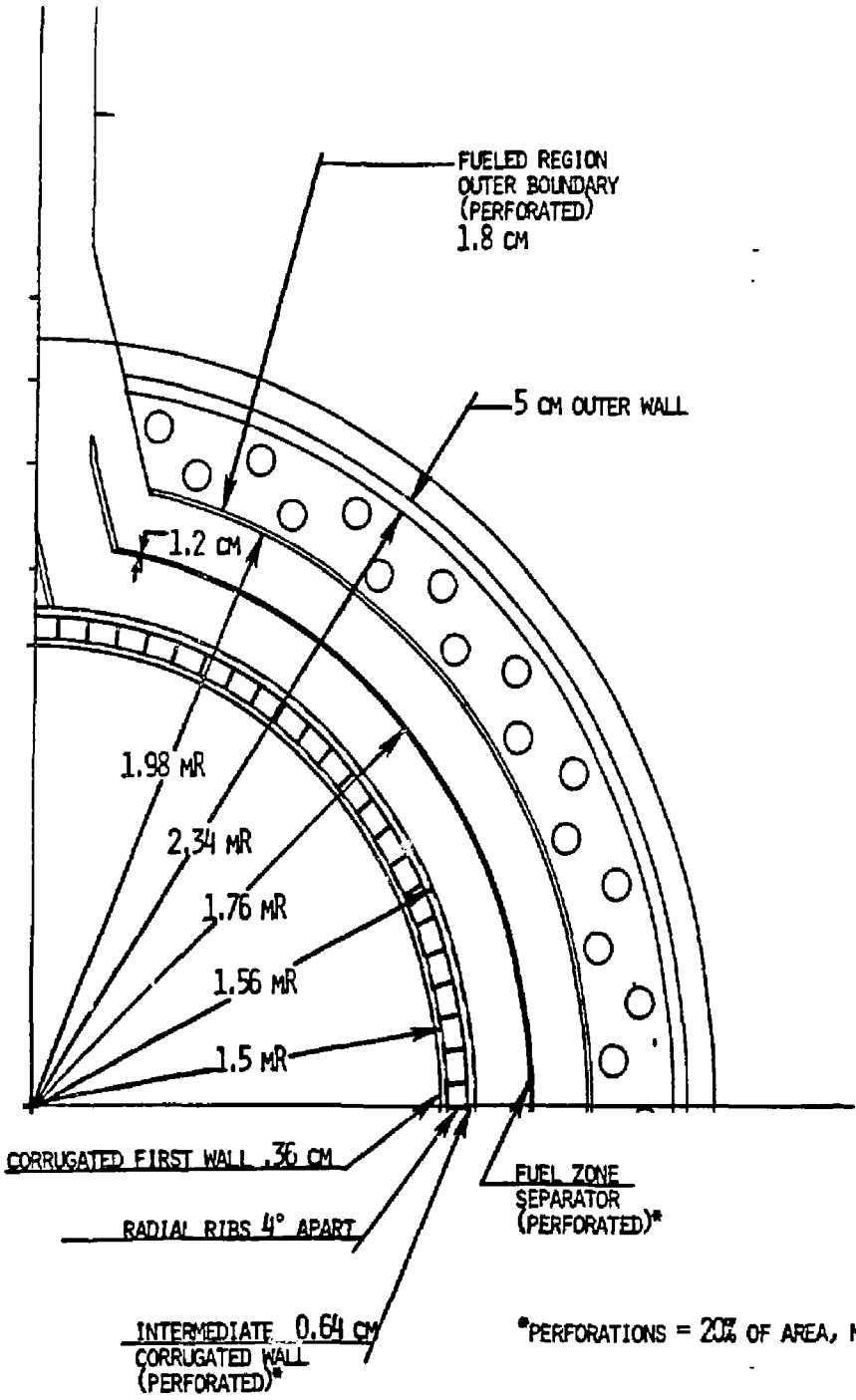


Figure 8.

Structural Dimensions for the Reference Fusion Breeder

Blanket Concept (not to scale).

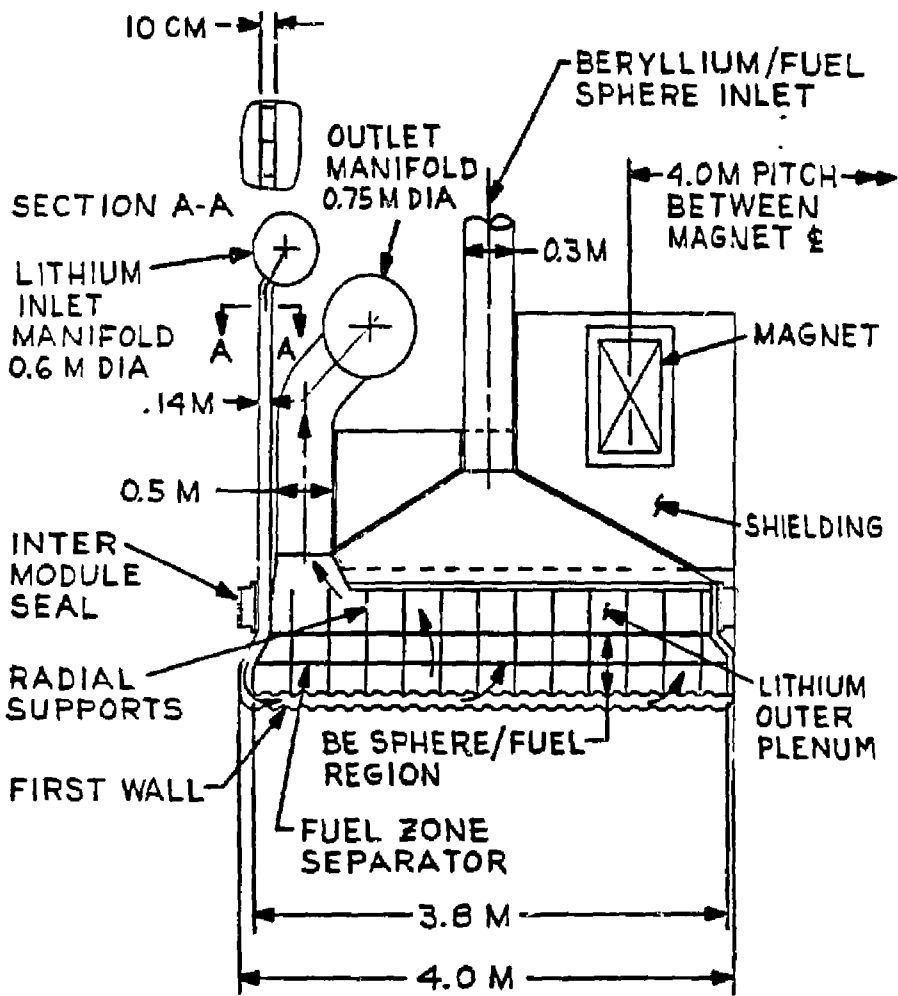


Figure 9.  
 Fusion Breeder Blanket Module  
 Cross Section - Top Portion of Module

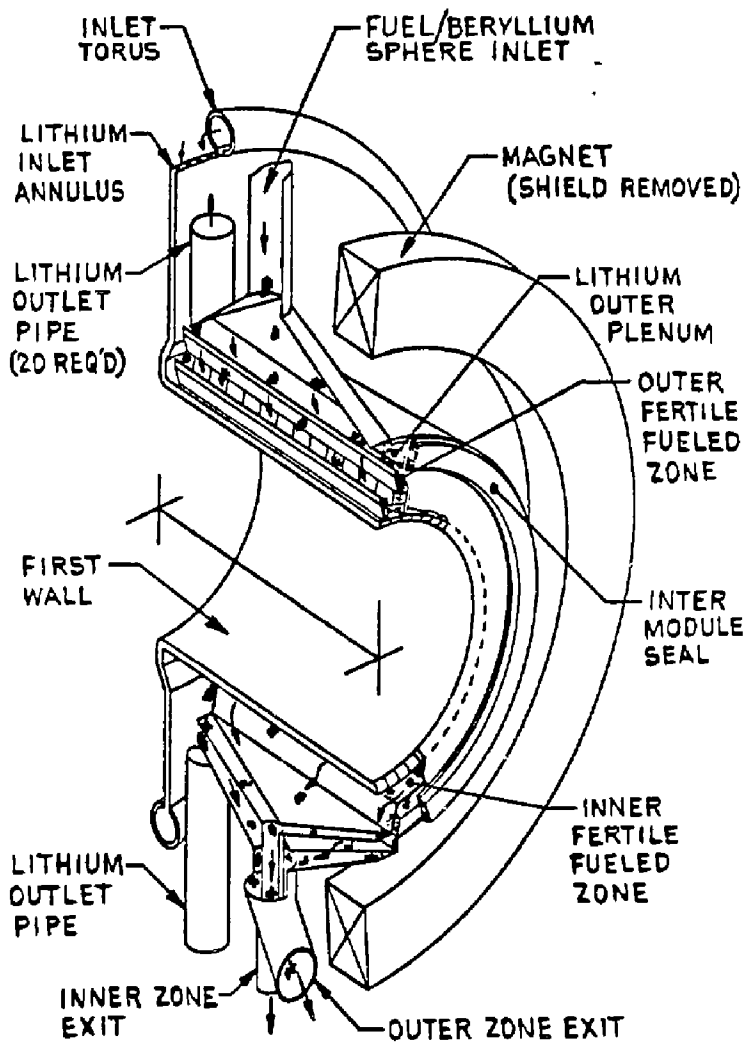


Figure 10.  
 Trimetric of Fusion Breeder Blanket Module Showing  
 Radial Zoning and Fuel Sphere Movement  
 Through the Blanket

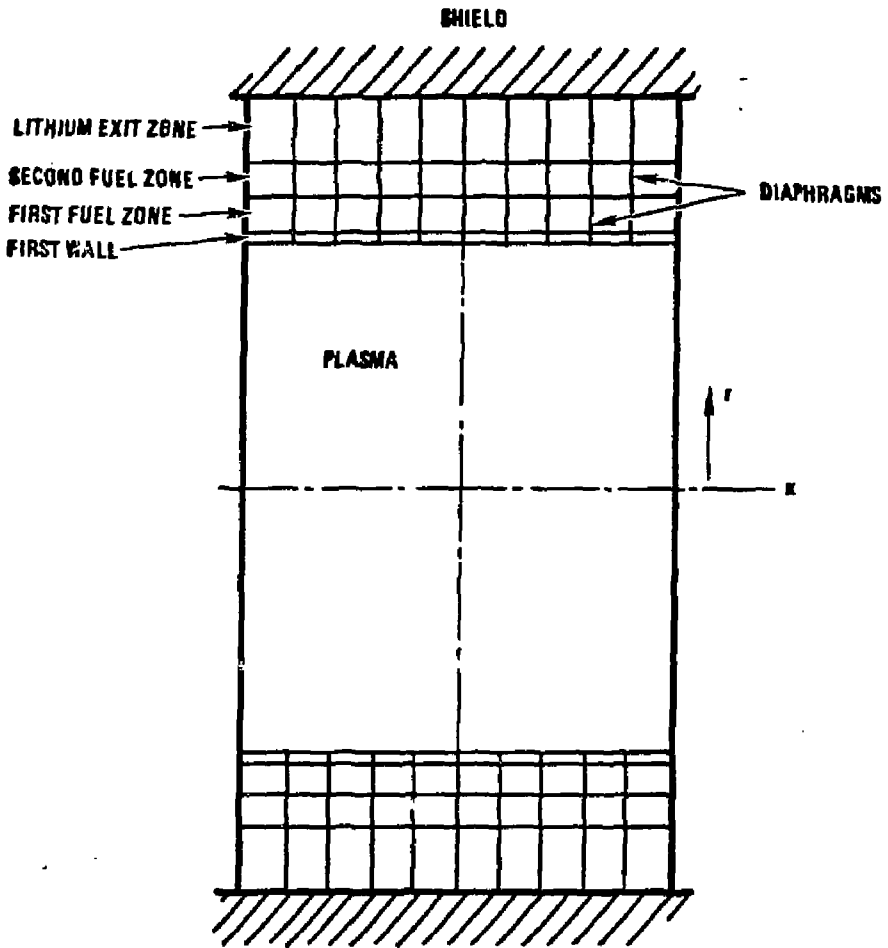


Figure 11.  
 Geometry and Coordinate System of Plate and Shell  
 Blanket Structural Model.

of the blanket are omitted (e.g., coolant and fuel inlets and outlets), but the essential features of the internal structure were included. Dead weight loads were ignored, but are not expected to significantly impact the stress levels.

The structural temperatures and coolant pressures associated with the current version of the reference blanket are compared with the earlier values in Figure 12. As shown, the coolant pressure loadings are somewhat higher than in the earlier version and the temperature differentials are somewhat greater. As a result, it is anticipated that stress levels will be substantially higher.

As shown in Figure 13, the initial evaluation of stresses in the earlier version of the reference blanket far exceeded the allowable stress level for HT-9 (approximately 175 MPa for <math>425^{\circ}\text{C}</math> operation with negligible thermal creep). However, it was found that two features of the initial model led to the high stress levels:

- The first and intermediate wall were modeled as two independent walls rather than as a composite.
- The radial support plates were rigidly connected to the outer wall of the blanket.

The composite wall not included in the initial stress model, but has been anticipated in the design and does not imply a significant design change. The effect of rigid connections to the outer wall was not anticipated in the earlier design and does imply a significant change in the current mechanical design.

As shown in Figure 14, with a composite first wall/intermediate wall and with a decoupled back wall, the stress levels for the earlier design can be reduced to below the allowables in all locations<sup>a</sup> except the module side

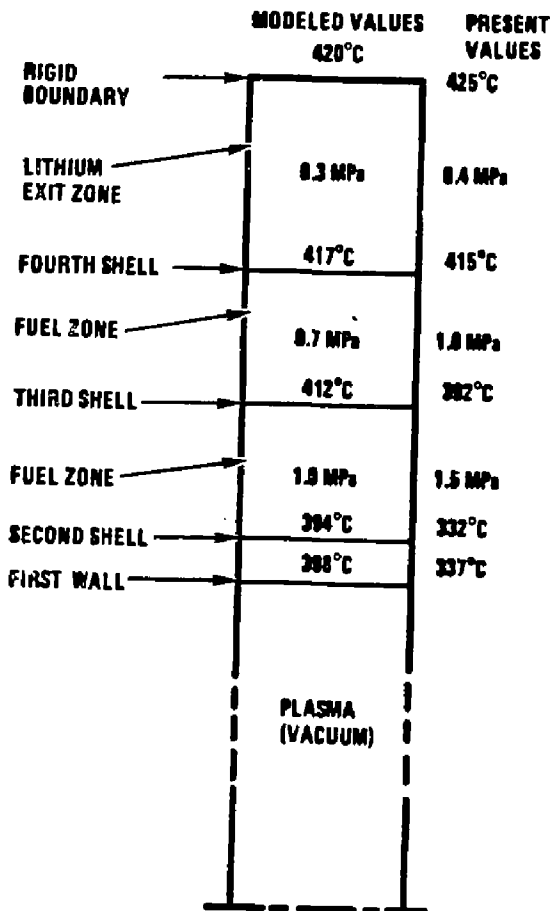


Figure 12.

Comparison of the Pressure and Thermal Loads Used in the Structural Model with Those of the Updated Reference Design.

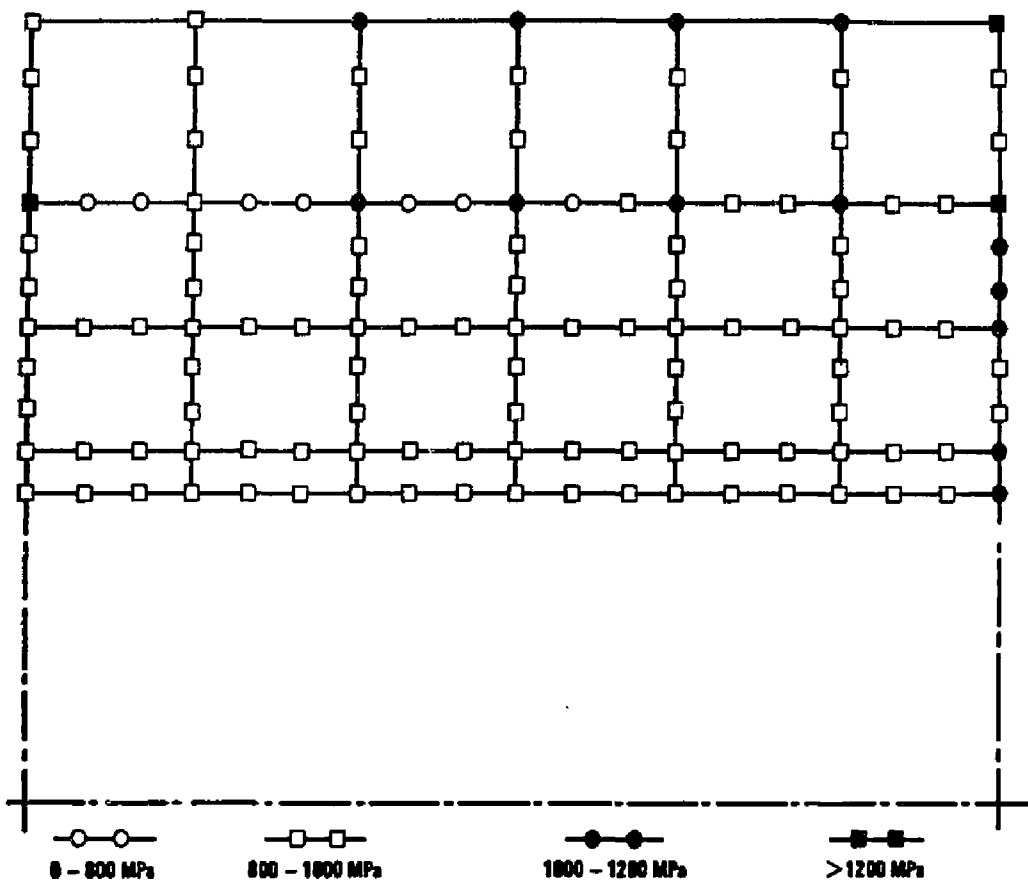


Figure 13.

Stress Map for Earlier Reference Design with Independent  
 First Wall and Rigidly Connected Back Wall.

<sup>a</sup>It should be noted that the intermediate wall stresses, which fall between 110 and 160 MPa on Figure 14, are near the lower bound at the first wall. This side wall was modeled as a 4 cm thick flat plate, but would be replaced by an ~1/cm thick elliptical end closure which would translate most of the bending stress to membrane stress.

These more encouraging results for the earlier design are expected to translate to the current design, despite its higher loading. Specifically, the thermal stresses can be almost eliminated by decoupling the back wall, and the pressure stresses are expected to be approximately 1.5 times as large, within the allowable limit of 175 MPa.

A potential design solution which accomplishes the goal of decoupling the interior structure of the blanket is shown in Figure 15. This modification preserves the blanket fuel zoning, but features three nested mechanical assemblies: a first wall/second wall composite with a split (to reduce thermal stress) diaphragm defining the first fuel zone, a third wall with a split concentric diaphragm (second fuel zone), and a fourth wall and split diaphragm (lithium outlet plenum). The entire internal assembly is supported by gravity (close tolerance not required) and fabrication of the modular blanket should be much easier. This improved option (or a similar variant) will replace the original blanket internal structure of the reference design.

#### III.D. Beryllium/Thorium Pebble Fuel Element

In this section, issues related to the use of beryllium/thorium fuel elements are reviewed. These issues include beryllium resources, fuel element design options, lifetime considerations, and fabrication technologies. These

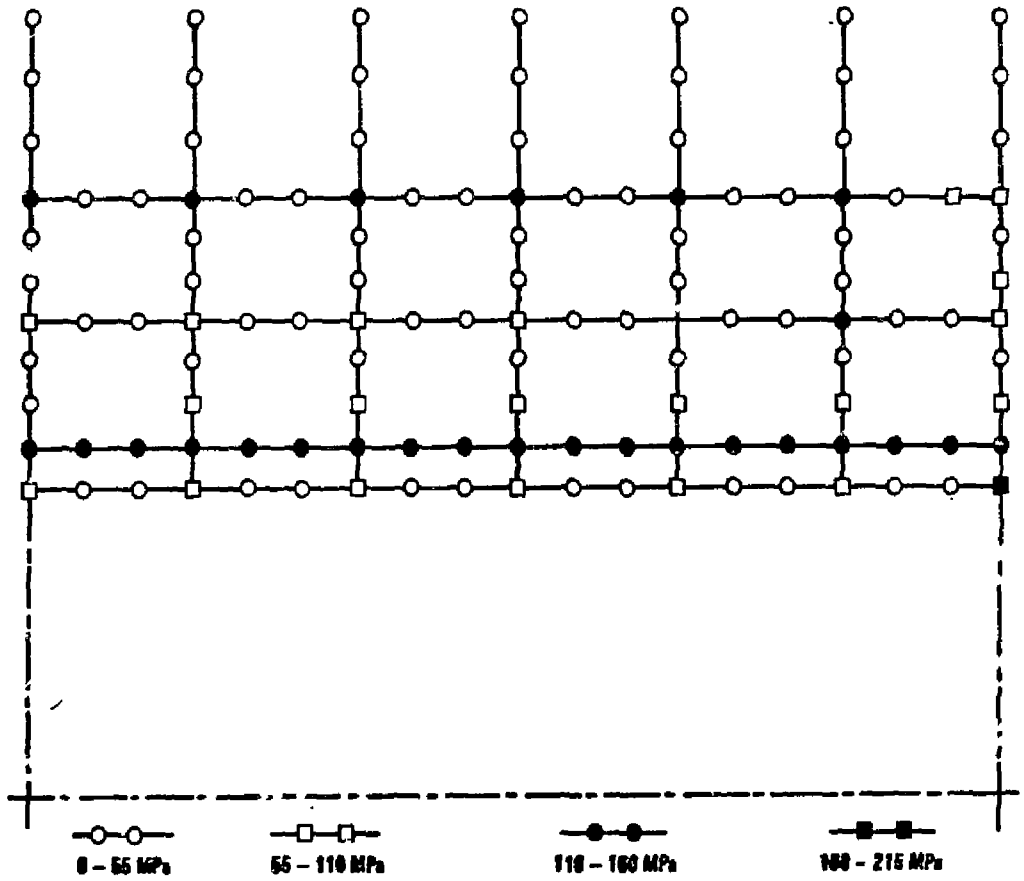


Figure 14.

Stress Model for Earlier Reference Design with Composite  
 First Wall/Intermediate Wall and Decoupled Outer Wall.

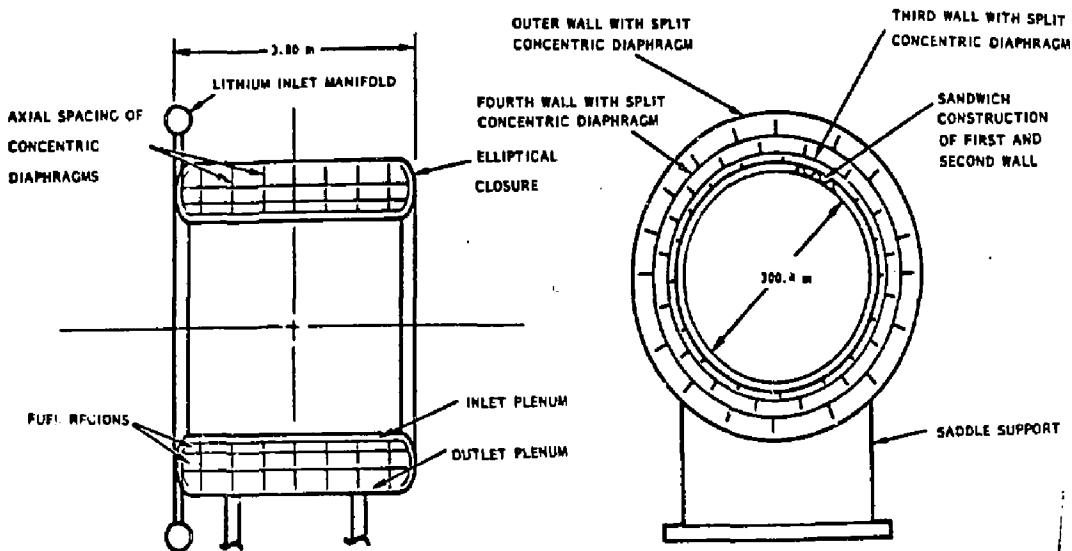


Figure 15.

A Design Solution Which Decouples the Entire Interior Structure is Expected to Provide Both Low Stress and Design Simplicity.

topics are described in more detail in References 2, 5, 8, 9, and 29.

### III.D.1 Beryllium Resources

Recent estimates of economically recoverable beryllium resources are shown in Table VII.<sup>(29)</sup> When compared with an expected cumulative U.S. beryllium usage by the year 2000 of only 8000 MT, it is clear that a large fraction of the beryllium resource will be available for fusion applications.

The beryllium requirements for the reference fusion breeder are given in Table VIII and are compared with the resource estimates in Table IX. Without recycle, the beryllium throughput is so large that beryllium makeup requirements can seriously impact resource availability. Beryllium will have to be recycled and losses cannot exceed a few percent for long term service (e.g., over 200 years).

Estimates of the electric power generation capacity which can be supported by half of the nominal domestic resources are shown in Table X. These estimates indicate that, with efficient recycle, fusion breeders using beryllium multiplier blankets can easily support over 1000 GW<sub>e</sub> of electric power production (including their own) for over 200 years into the future - a period roughly corresponding to the period from the beginning of the industrial revolution until today.

### III.D.2 Pebble Design Considerations

Three beryllium/thorium composite fuel candidates are shown in Figure 16. Each has advantages and disadvantages. Candidate A, a solid thorium pin, which is nested in the core of the beryllium pebble using alloy steel clips, has the advantage of separating the beryllium and thorium (small lithium filled gap), thus limiting possible intermetallic compound (Be<sub>13</sub>Th)

Table VII.  
Beryllium Resource Data

	(Metric Tons)			
	United States		World <sup>b</sup>	
	Reserves	Resources <sup>a</sup>	Reserves	Resources <sup>a</sup>
U.S. Bureau of Mines	25,000	73,000	530,000	1,535,000
U.S. Geological Survey	55,000	282,000	234,000	1,110,000
Nominal Estimate	55,000	150,000	300,000	1,180,000

<sup>a</sup>Includes Reserves

<sup>b</sup>Includes U.S.

Table VIII.  
Beryllium Requirements for the Reference Fusion Breeder

Total fuel zone volume	550 m <sup>3</sup>
Beryllium/thorium pebble volume	330 m <sup>3</sup>
Beryllium/thorium pebble quantity	23 · 10 <sup>6</sup>
Beryllium volume	242 m <sup>3</sup>
Beryllium mass	445 MT
Average beryllium residence time <sup>a</sup>	1.65 yr
Annual pebble throughput <sup>a</sup>	14 · 10 <sup>6</sup> yr <sup>-1</sup>
Annual beryllium mass throughput <sup>a</sup>	265 MT/yr

a) conservative. Assumes beryllium refurbishment following each pass through the blanket

Table IX.  
Summary of Contributions to Beryllium Requirements  
for the Reference Fusion Breeder

	Annual (MT/yr)	30-Year Life Cycle (MT)	As Fraction of Nominal Domestic Resource (%)
Initial inventory	--	450	0.30
Burnup	0.4	11	0.01
Makeup (1.65 yr life)			
No recycle	265	7,950	5.30
Recycle (7% loss)	19	560	0.37
Recycle (1% loss)	2.7	52	0.05

Table X.  
Results of the Beryllium Resource Assessment  
for Fusion Breeder Applications  
[U.S. Electrical Capacity Which Can Be Supported (GW<sub>e</sub>) by  
Domestic Resources]

Beryllium Lifetime (yr)	Fusion Economy Duration (yr)	Without Recycle	With Recycle Loss of		
			7%	1%	0%
1	30	131	1026	1824	2095
	60	69	679	1065	2079
	200	21	262	1030	2013
2	30	255	1645	2535	2785
	60	133	1164	2307	2760
	200	41	490	1624	2640
5	30	587	2583	3312	3475
	60	320	2040	3128	3434
	200	104	1030	2486	3252
10	30	1030	3186	3687	3786
	60	593	2723	3549	3738
	200	200	1624	3020	3524

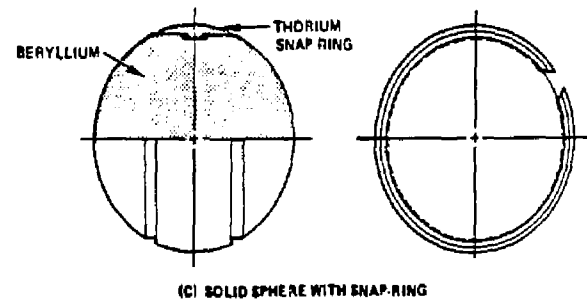
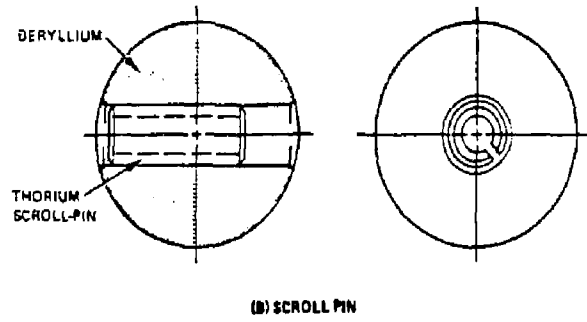
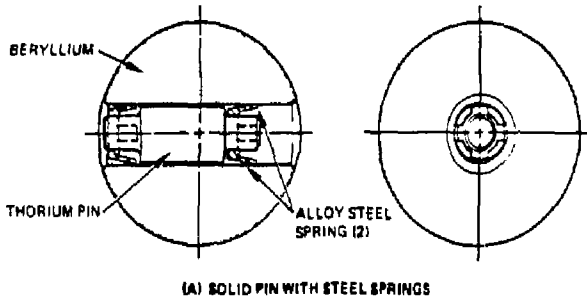


Figure 16.  
Several Beryllium/Thorium Pebble Designs.

formation between the two metals.<sup>(2)</sup> However, the large heat generation in the thorium clip drives a temperature gradient from the center to the outer surface of the beryllium pebble, possibly shortening the beryllium lifetime by causing differential swelling induced stresses.

The scroll pin fuel form (candidate B) has the advantage that the steel clips (which raises mass transfer issues of their own) are eliminated, but does not seek to inhibit the Be-Th interaction and continues to drive heat through the beryllium pebble.

The snap-ring fuel form (candidate C), which was selected as a baseline, also places beryllium in contact with thorium, but maintains a very uniform temperature profile in the beryllium pebble (see Figure 17). If Be-Th interactions are shown to be excessive, then a diffusion barrier (e.g., molybdenum on thorium or TiC on beryllium) should be investigated. It would also be possible to adapt the alloy spring to an outside thorium ring. The beryllium/thorium fuel element, sized for current reference conditions, is shown in Figure 18. The pebble consists of 27 volume percent thorium in a 3.5 mm thick ring. The maximum temperature difference for a pebble at the front of the blanket is 40°C.

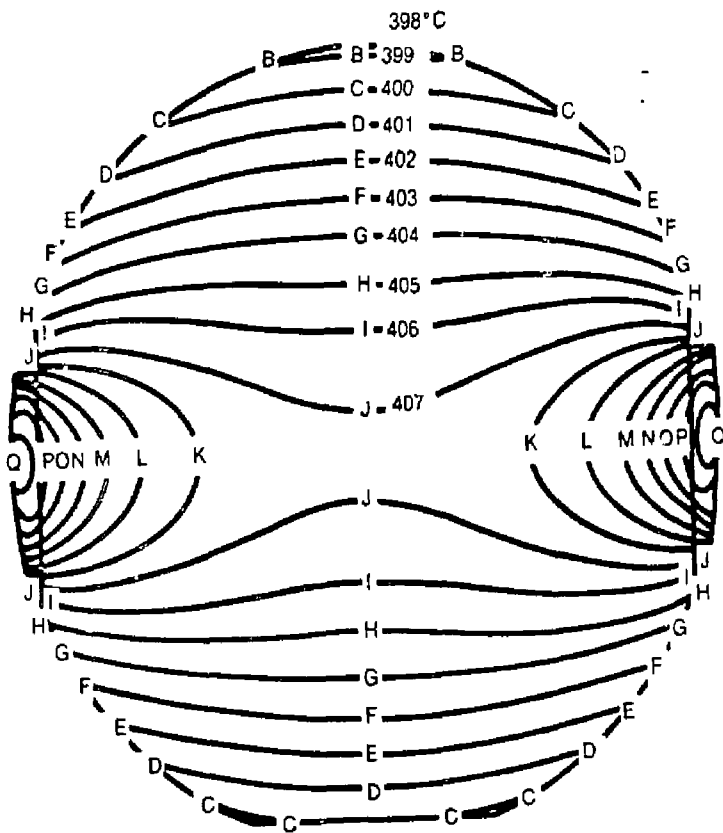
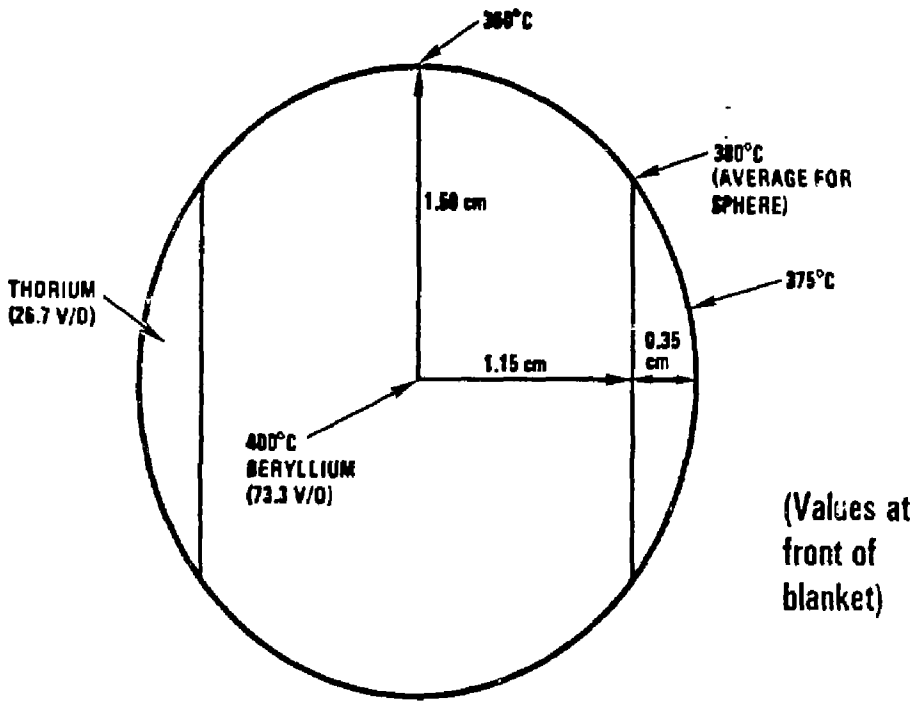


Figure 17. Beryllium/thorium snap ring fuel element  
isoplot



	Volume	Mass
Beryllium	10.4	19.1 (at 1.84 g/cm <sup>3</sup> )
Thorium	3.7	43.3 (at 11.7 g/cm <sup>3</sup> )
Total	14.1 cm <sup>3</sup>	62.4 g

Figure 18.

The Beryllium/Thorium Pebble Modified to Accommodate the Increased Thorium Fraction of the Current Reference Design.

### III.D.3 Beryllium Lifetime

In a functional sense, the beryllium lifetime must exceed the fuel residence time (315 full power days in inner fuel zone, 630 full power days in outer zone). These minimum requirements imply a radioactive beryllium recycle rate of 265 MT/yr, or 14 million 3 cm O.D. pebbles per year or 0.5 pebbles/second. This requirement is within the realm of developable technological capability for automated fabrication of low tolerance parts<sup>(9)</sup> and is not expected to be prohibitively expensive (roughly \$40 million in direct capital cost for process plant with above capacity), but a longer lifetime will reduce the throughput, providing some advantage.

The lifetime of a beryllium pebble is determined by some combination of the effects listed below:

- Corrosion in the lithium/thorium/steel environment.
- Thermally induced differential swelling.
- Loss of ductility.

The first of these was mentioned earlier and appears to be amenable to solution. The second and third effects can work together to result in pebble cracking and possible failure.

More specifically, beryllium pebbles are expected to swell at the rate indicated in Figure 19.<sup>(9)</sup> As shown, the threshold temperature for high swelling occurs between 300°C and 500°C depending upon the helium dose. For the reference blanket conditions, a 316 full power day residence time at a 1.7 MW/m<sup>2</sup> neutron wall load will result in about 5600 appm helium production in the front of the blanket,<sup>(5)</sup> where the peak temperature will be 400°C and the minimum beryllium temperature (Figure 18) will be 360°C. The volumetric swelling for each position will be low (about 0.3 percent ( $\Delta V/V$ )) and will be nearly identical. Therefore, in the reference design regime thermally induced

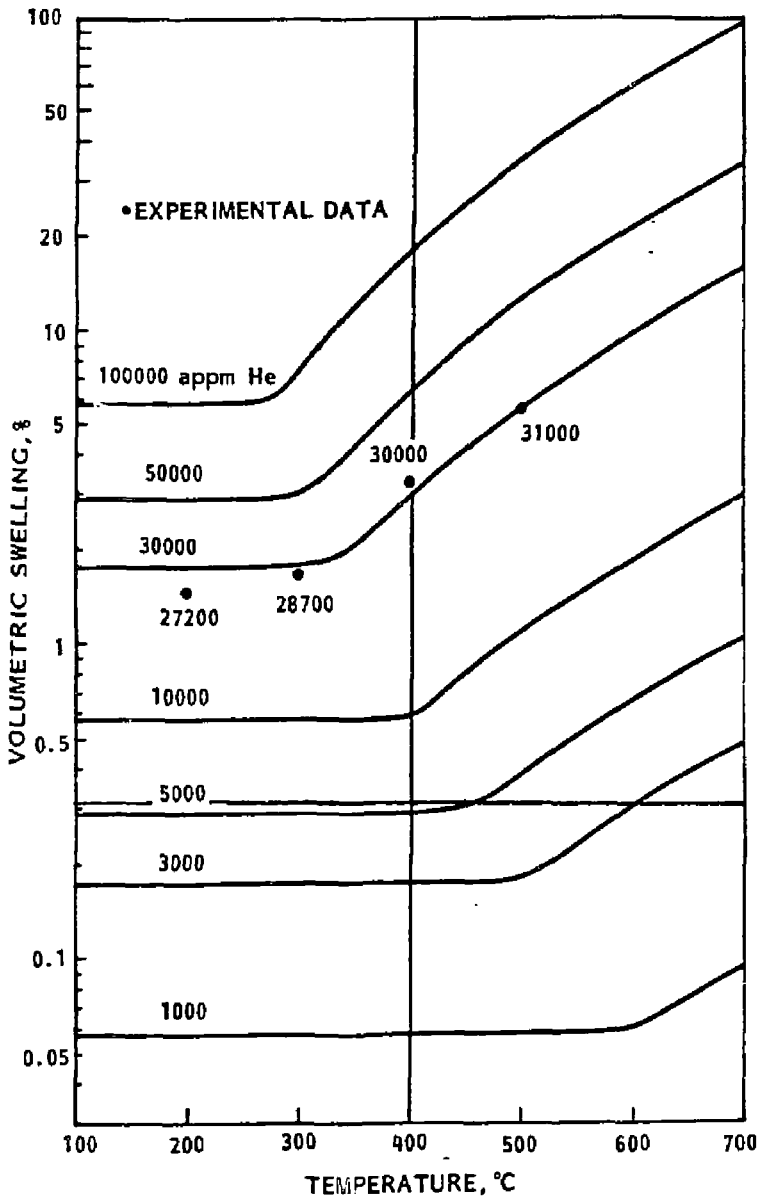


Figure 19.

New Theoretical Models of Beryllium Swelling  
 versus Temperature and Fluence.

differential swelling is not expected to be an issue. This conclusion also holds for the outer fuel zone, where temperatures are higher but closer together and the helium production rate is much lower.

If, however, we strive for a longer lifetime of, perhaps, 5 full power years, then the situation becomes more complex. Specifically, for the above conditions, the helium generation would be about 30,000 appm and temperature induced differential swelling stresses will become important above about 350°C. In such cases, it is believed that the core of the pebble will swell more, expanding the outer skin until it cracks due to fracture toughness limits. Very conservative models of this mechanism have been used to estimate an average-over-blanket beryllium lifetime in excess of 3.4 full power years (over twice assumed lifetime), assuming a 50 percent stress relaxation due to thermal and/or irradiation creep. Higher fracture toughnesses than assumed ( $12 \text{ MPa} \cdot \text{m}^{1/2}$ ), or stress relief due to shallow cracking are additional mechanisms which could further extend the beryllium lifetime. This failure mechanism is highly interactive and requires in-core fission testing to better understand the failure mode.

### III.E. Reactor Safety

In this section, reactor safety considerations for the reference fusion breeder blanket are reviewed. Safety goals and objectives are discussed, the features of several reactor safety systems are defined, and the results of a preliminary probabilistic risk assessment are discussed. It should be noted that the later activity was performed with an eye towards identifying those accident scenarios which deserve increased attention rather than as an exercise to provide a quantified estimate of the integrated risk. Safety topics are described in more detail in References 2, 5, and 6.

### III.E.1 Safety Requirements and Goals

In comparison with fusion-electric power generation, fusion breeders are characterized by higher radioactivity inventories and higher decay afterheat levels. However, fusion breeder safety must be considered in the context of the overall fusion-fission electricity generation. Specifically, the following system level features should be noted:

- The much larger electricity generation system would be dominated by fission reactors.
- The fusion breeder could be located far from population centers in dedicated fuel cycle centers.

Thus, a logical overall requirement for fusion breeder safety is that it not detract from the safety of the entire fission reactor dominated system. In practice, this implies that the integrated risk (measured in Rem/kW<sub>e</sub>-H) should be roughly equal to, or less than that of the client fission reactors (e.g., LWRs). In contrast, fusion-electric reactors, which are likely to be located near population centers and are likely to be substantially more expensive than fission reactors, must provide demonstrated safety and environmental advantages. These advantages can include some combination of "passive" safety, low radio-nuclide inventory, low activation structural materials, etc.

Although safety requirements are relaxed for the fusion breeder relative to the fusion-electric application, ambitious safety goals have been established. These include the use of multiple, redundant safety systems and the use of one or more passively cooled fuel dump tanks as an ultimate safety system.

### III.E.2 Safety Issues, Design Features, and Subsystems

The leading causes for concern regarding blanket safety are those mechanisms by which "stored energy" can result in the release of radioactive products into the environment. Four potential sources of stored energy have been identified.

- Nuclear energy which might be released if the reactivity of  $^{233}\text{U}$  in the thorium fuel were to increase.
- Mechanical stored energy due to helium production in the irradiated beryllium which can be released via pebble expansion if blanket temperatures become excessive.
- Chemical stored energy in the liquid lithium coolant which can be released in the event of a lithium fire.
- Nuclear decay afterheat in the fuel (see Figure 2) and structure which is continuously released after shutdown.

Each of these energy sources is discussed in the following subsections. Design features and safety subsystems which are intended to limit the possibility of radioactive release are also reviewed.

#### III.E.2.a Nuclear Reactivity/Criticality

There is a concern that, should some or all of the lithium coolant (which is a strong neutron absorber) be removed from a blanket module (either by leak or faulty procedure), then the reactivity of the remaining beryllium/thorium/ $^{233}\text{U}$  pebble bed will increase. This situation is easily controllable (e.g., reactor trip on excessive coolant outlet temperature), except when the  $^{233}\text{U}$  concentration is so high that, in the absence of the lithium coolant, the criticality coefficient,  $K_{\infty}$ , exceeds 1.0. For the reference fusion breeder blanket, neutronics calculations indicate that a  $^{233}\text{U}$

discharge concentration below 5 percent is expected to satisfy the above subcriticality requirement. Thus, criticality is not an issue.

### III.E.2.b Pebble Expansion

A rapid increase in the blanket temperature could lead to a rapid increase in beryllium volume which could conceivably lead to a fuel blockage and/or rupture of the contents of one or more blanket modules. As indicated in Figure 19, this concern may not be important for the reference conditions (approximately 5600 appm (maximum)) because the net linear expansion for a blanket temperature excursion to 900°C (for which structural integrity is assumed to be lost in any case) would result in a linear growth ( $\Delta L/L$ ) of less than 0.5 percent, or only 0.2 cm across the entire blanket zone. Pebble expansion would become a serious issue if an ~5 yr beryllium lifetime were specified.

### III.E.2.c Lithium Fire

The consequences of a lithium fire could be the failure of an overheated structure, with the consequent release of volatile oxides and other radioactive constituents. Although the potential for lithium fires is a concern, the design philosophy is to borrow techniques for active and passive liquid metal fire protection which have been developed for the sodium cooled LMFBR. A number of engineered safety features can be invoked, including the following:

- Use of an inert gas environment.
- Use of steel-lined concrete chambers with sacrificial material between the steel liner and the concrete.
- Use of deep, narrow sumps with sloped surfaces leading to dump tanks

which collect any spilled lithium in the reactor building.

- Use of steel balls and hollow graphite microspheres in spillage areas to rapidly cool and choke any spilled lithium.
- Active chemical fire fighting techniques.

Using a combination of the above, with the required procedures and instrumentation, it is believed that the risk of a lithium fire can be ameliorated. It should be noted that the plant would also employ a sodium intermediate loop to limit radioactive releases as well as any lithium/water interface. There would be no water cooled equipment in the reactor building.

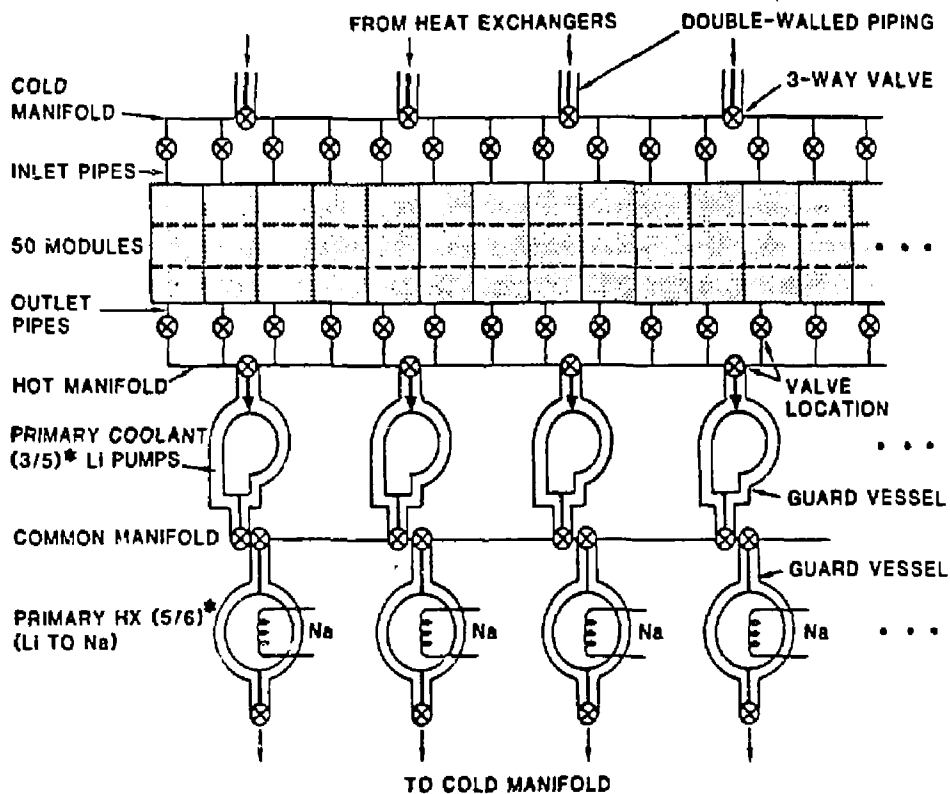
#### III.E.2.d Nuclear Decay Afterheat

The failure of one or more nuclear decay afterheat removal systems can result in the failure of an overheated structure with the consequent loss of its radioactive contents. Afterheat, a natural consequence of nuclear absorption processes, cannot be "designed away," but must be accommodated by providing a combination of the following features:

- Ability to isolate failed component.
- Redundant cooling systems.
- Alternate heat flow paths.
- Ability to provide for stable geometry.

As shown in Figure 20, the primary loop of the fusion breeder would incorporate redundant capabilities (any combination of blankets, pumps, and heat exchangers is possible) and oversized components (e.g., only 3 of 5 lithium pumps required to operate at full capacity). If required, any failed component can be isolated from the system.

In cases for which a blanket module is subject to a loss of primary coolant flow (LOCF) or a loss of coolant accident (LOCA), alternate heat flow



\* (REQUIRED NUMBER OF COMPONENTS/NUMBER OF COMPONENTS AVAILABLE)

Figure 20.

Fusion Breeder Primary Loop Logic.

paths will be required to remove the decay heat. Three alternate flow paths have been considered:

- Coolant flow through the pebble handling circuit.
- Heat conduction to a cooled shield.
- Heat conduction through the first wall using an auxiliary first wall cooling system.

The first of these involves using the pebble handling circuit (Figure 3) to circulate sufficient lithium coolant to continue to cool the blanket after the fusion neutron source is shutdown. It can be accomplished using the independent pump and heat exchanger capacity that are built into the pebble handling circuit, but requires that the blanket coolant boundary (e.g., first wall) retain its integrity and is not suitable for some LOCA situations.

The second and third of the above heat flow paths are available in both LOCF and LOCA situations. Decay heat removal using the shield involves the use of an independent shield cooling system (lithium or other coolant compatible with blanket coolant) which is maintained near the blanket coolant outlet temperature of 425°C. In this case, as the blanket temperature increases beyond the outlet temperature, heat is conducted and (if the fuel and/or coolant are absent) radiated to the cooler shield.

The auxiliary first wall cooling system is assumed to consist of a large fan(s) located near the end of the central cell. In the event of an accident, these fans (which are comparable in power rating to small airplane engines), would circulate the reactor building cover gas through the central cell to cool the first wall (maximum required velocity approximately 50 m/s).

A final mechanism for removing decay afterheat is to dump the contents of the blanket to a separately (and probably passively) cooled dump tank located below the blanket. As shown in Figure 3, one such tank might be provided for

each five blanket modules. The same tank would also be used for fuel management operations. The act of dumping can be performed semi-passively. That is, a modest refrigerator coil under each module can be used in normal operation to freeze a solid lithium plug (m.p. =  $190^{\circ}\text{C}$ ) in the dump line. If the fuel is to be dumped, a loss of refrigerator power will cause the plug to quickly melt and the fuel to gravity dump. Either natural convection or heat pipes can be used to possibly cool the dump tanks (5).

### III.E.3 Safety System Modeling

Time dependent thermal models of the blanket during four major accident scenarios have been developed. (2,5) These models included LOCF and LOCA cases for which the beryllium/thorium pebbles can and cannot be dumped to an independently cooled dump tank. The results, summarized in Table XI, indicate that shield cooling alone is adequate to maintain blanket structural integrity for blanket module reuse (temperature for reuse limited to below  $730^{\circ}\text{C}$  ferritic steel recrystallization phase change temperature) in all cases except the LOCA case in which the pebbles are not dumped.

In this worst case, shown in Figure 21, operation of the auxiliary first wall cooling system in addition to shield cooling appear to be marginally adequate in the sense that the  $730^{\circ}\text{C}$  limit for reuse will be exceeded. However, despite internal temperatures in the  $900$  to  $1000^{\circ}\text{C}$  range, the outer blanket boundaries is expected to remain cool enough to prevent a gross deformation of the blanket structure.

Table XI.

## Safety System Capabilities for Various Accident Scenarios

	Shield Cooling Alone	Auxiliary First Wall Cooling Alone	Both Systems
Loss of coolant flow, fuel not dumped	Adequate	Not adequate	--
Loss of coolant flow, fuel dumped	Adequate	Adequate	--
Loss of coolant, fuel not dumped	Not adequate	Not adequate	Marginal <sup>a</sup>
Loss of coolant, fuel dumped	Adequate	Adequate	--

<sup>a</sup>Exceeds 730°C limit for reuse in approximately 2 hours. Blanket intervals temperature may exceed 900°C limit for structure integrity if steel emissivity is less than 0.5. Further analysis required.

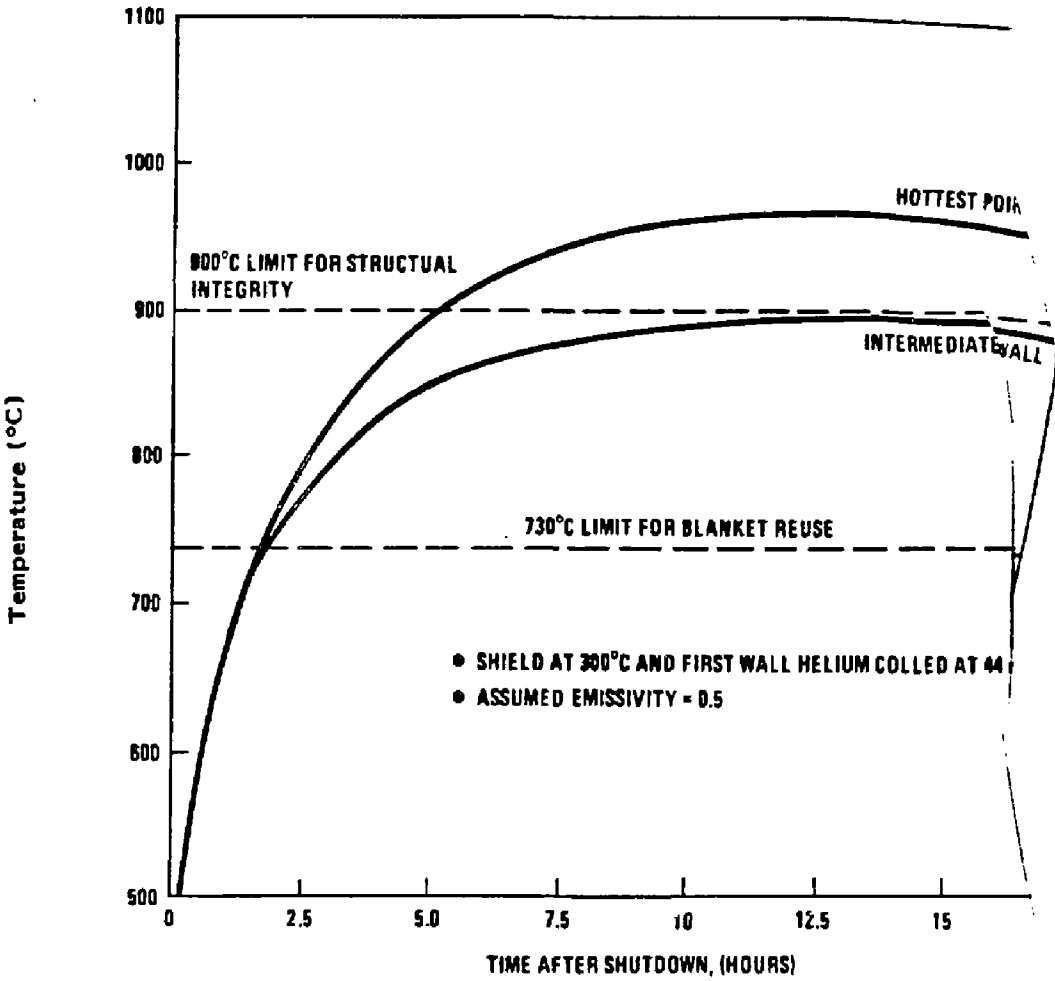


Figure 21.

Thermal Modeling Results for Loss of Coolant Accident with Fuel in Place (Worst Case for the Afterheat Cooling Systems).

#### III.E.4 Results of Probabilistic Risk Assessment

A probabilistic risk assessment (PRA) was performed for the reference design to identify potentially high risk failure modes. This assessment, discussed in more detail in Reference 5, included the following considerations:

- Radioactive inventories (e.g., activated structure, tritium, actinides, fission products in coolant).
- Capabilities of safety systems.
- Component failure probabilities (e.g., valves).
- Event trees leading to releases.
- Radiological consequences of release.

Previous fission reactor experience and analysis were used to develop many of the expected probabilities and consequences.

One event tree, starting with a first wall failure, is shown in Figure 22. As shown, if the primary safety systems (dump valve, module isolation valves, shield coolant) function, the consequence is small, but the probability (1%/year) is relatively large because the first wall is expected to be a weak link in the system. The branches with the highest consequence are D8 and D10, but these require secondary containment failure, have probabilities in the range of  $\epsilon < 10^{-9}\text{yr}^{-1}$  per year and are not considered to be credible. The branches with the next highest consequences are D7 and D9. In both cases the failed module is isolated, but the dump valve fails, and either the shield cooling system or the auxiliary first wall cooling system fails. Consequently, the radioactivity associated with one module would be released to the containment building.

FIRST WALL FAILS	DUMP VALVE OPENS	FAILED MODULE ISOLATED	SHIELD COOLING SYSTEM FUNCTIONS	AUXILIARY FIRST WALL COOLING SYSTEM FUNCTIONS	SECONDARY CONTAINMENT FUNCTION	BRANCH ID	PROBABILITY (PER YEAR)	CONSEQUENCES (REM)			
$10^{-2}/y$	~1	~1	~1			D1	$10^{-2}$	$3 \times 10^{-8}$			
			$10^{-3}$	~1		D2	$10^{-5}$	$3 \times 10^{-8}$			
				$10^{-3}$	~1		D3	$10^{-8}$	$2 \times 10^{-5}$		
					$10^{-4}$		D4	$c(10^{-12})$	1		
							D5	c	-		
							D6	$10^{-5}$	$3 \times 10^{-8}$		
					$10^{-3}$	~1		D7	$10^{-8}$	$8 \times 10^{-2}$	
						$10^{-4}$		D8	c	00	
							$10^{-3}$	~1	D9	$10^{-4}$	$8 \times 10^{-2}$
							$10^{-4}$		D10	c	00
									D11	c	-

Figure 22.

Typical Event Tree Used in Probabilistic Risk Assessment

Three other event initiators were assessed: (1) module inlet/outlet distribution plenum failures, (2) failures of all primary coolant pumps or intermediate heat exchangers, and (3) failures of the inlet/outlet piping or the cold or hot manifolds. The overall results are shown in Figure 23. The first wall failure (branch D1) discussed above is expected to provide the highest overall risk (probability x consequence). Other high risk branches involve an inlet/outlet piping failure (B1) and a complete coolant pump/IXH failure (A7). The piping failure is similar to the first wall failure but lower probabilities and higher consequences are assumed. The pump/IXH failure is a low probability-high consequence event that might be made to be inconceivable via use of emergency diesel backup generators.

It is important to emphasize that the PRA technique is viewed as a useful method to identify weak links in the system (e.g., the first wall), to set goal requirements (e.g., failure probabilities), and to establish a preferred safety system logic. For example, the severity of branches D7 and D9 of Figure 22 is greatly reduced by adding the shield and first wall coolant systems. This is indicated in Figure 23. The PRA is not expected to provide an absolute measure of the overall risk.

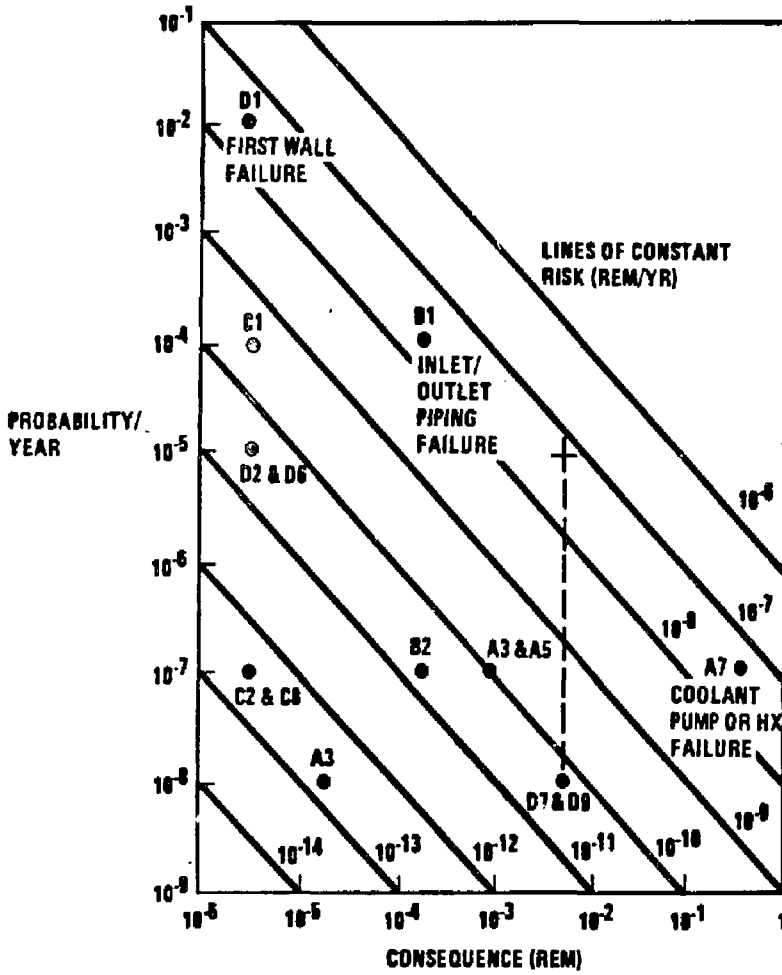


Figure 23.

Relative Risks of Various Accident Sequences.

#### IV. FUSION BREEDER PLANT CONCEPT

Although the fusion breeder program has emphasized the design of breeding blankets and associated technologies, there has also been an attempt to describe and cost the entire power plant. This integrated description of the plant cost and power flow can be used to provide a best estimate of the ultimate commercial merit of the fusion breeder application.

The plant design information developed in the section has been used to generate the systems and economics analysis described in Section VI.

##### IV.A Plant Overview

In this section, a top level description of the fusion breeder plant is described. The reader is reminded that the fusion reactor, which is central to the plant description, is nearly identical to that of the Mirror Advanced Reactor Study (MARS) described in detail in Reference 10. The MARS end plug, shown in Figure 24, has not been changed, although it is clear that the more recent octupole end-plug designs currently being pursued as part of the MINIMARS effort at LLNL (12), would provide some advantage if scaled to the higher power level of the fusion breeder.

The principal difference between the MARS and the reference fusion breeder plant (2) involve the nuclear, power conversion, and reactor safety systems of the plant. Although the central cell length and magnetic field strength are preserved, the use of the lithium cooled fusion breeder blanket design (MARS would be cooled using the Pb-Li eutectic) leads to changes in the following areas:

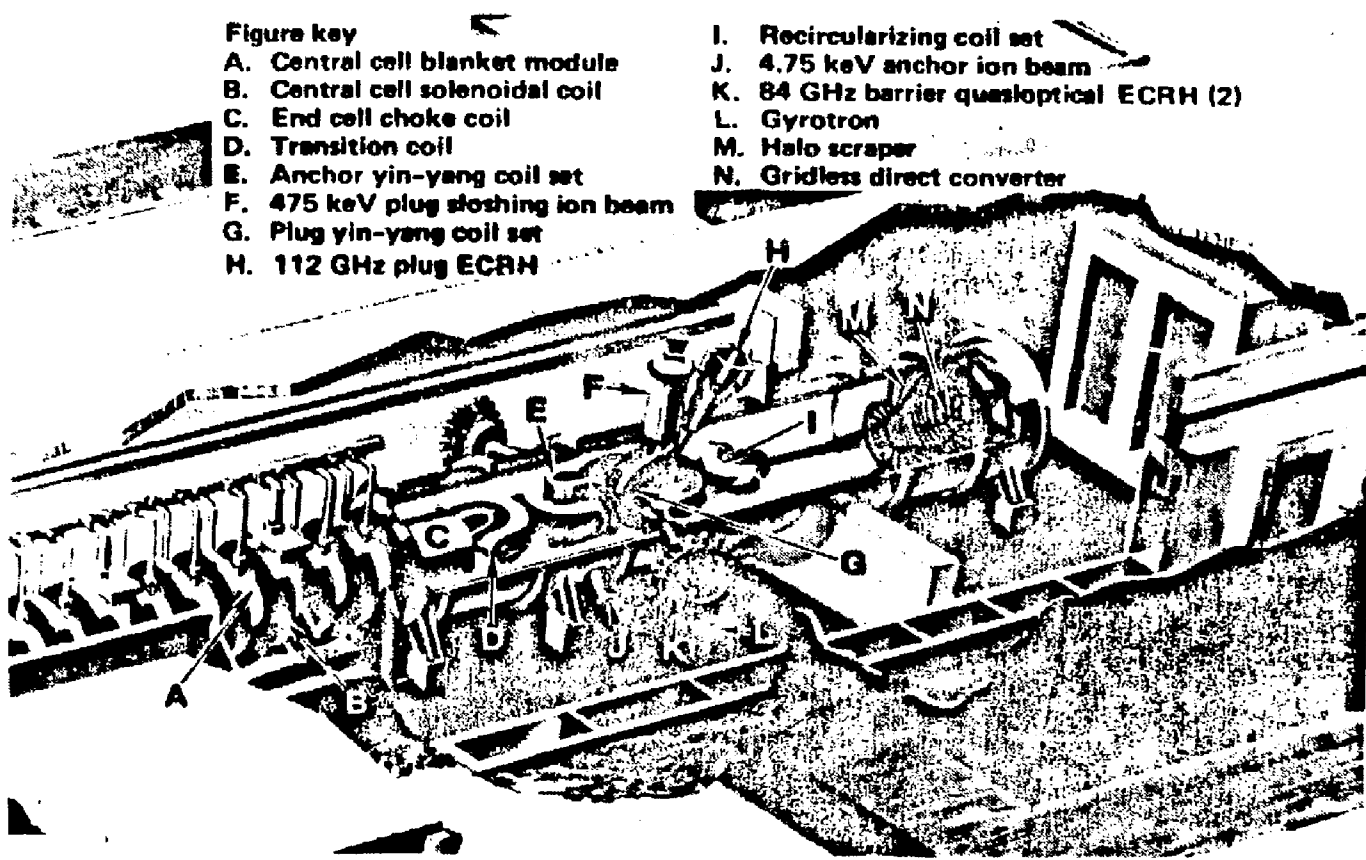


Figure 24.

MARS End Plug Technologies

- Blankets would be replaced by a horizontal, rather than vertical, translation. Thus, as indicated in Figure 25, all heat exchangers pumps, valves, etc. would be located on one side of the central cell, preserving the other side for maintenance operations.
- Recognizing the potential for the lithium-water reaction, water would be eliminated from the central cell building and a reasonably fast acting isolation barrier between the central cell and plug would be provided.
- As shown in Figure 25 and discussed in Reference 2, Li/Na intermediate heat exchangers and a sodium intermediate loop would be provided.
- A nuclear grade containment building and the safety/fuel management systems discussed in Sections II.A, III.A, and III.E would be provided. These would include provision to convey spent thorium and beryllium parts directly to adjoining process plants for reprocessing and refabrication, respectively. The latter facilities are also considered to be part of the fusion breeder plant (see Section V), but could be shared among more than one fusion breeder.

The above changes tend to increase the plant cost relative to MARS and are reflected in the cost estimates of Section IV.C

#### IV.B Integrated Power Flow Summary

The integrated power flow associated with the reference fusion breeder is summarized in Figure 26. In this figure, the plasma heating systems (RF heating, neutral beams) are lumped into one system providing 100 MW of power

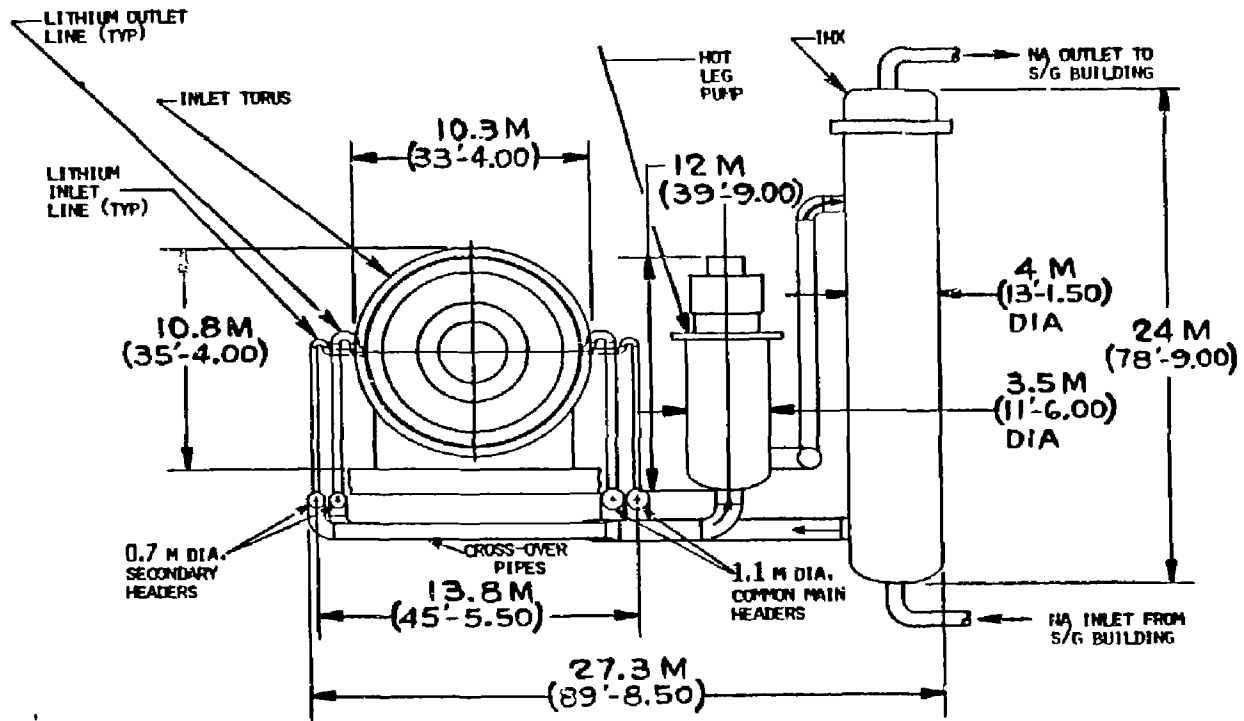


Figure 25. Central Cell and Component arrangement within the Fusion Breeder Reactor Building

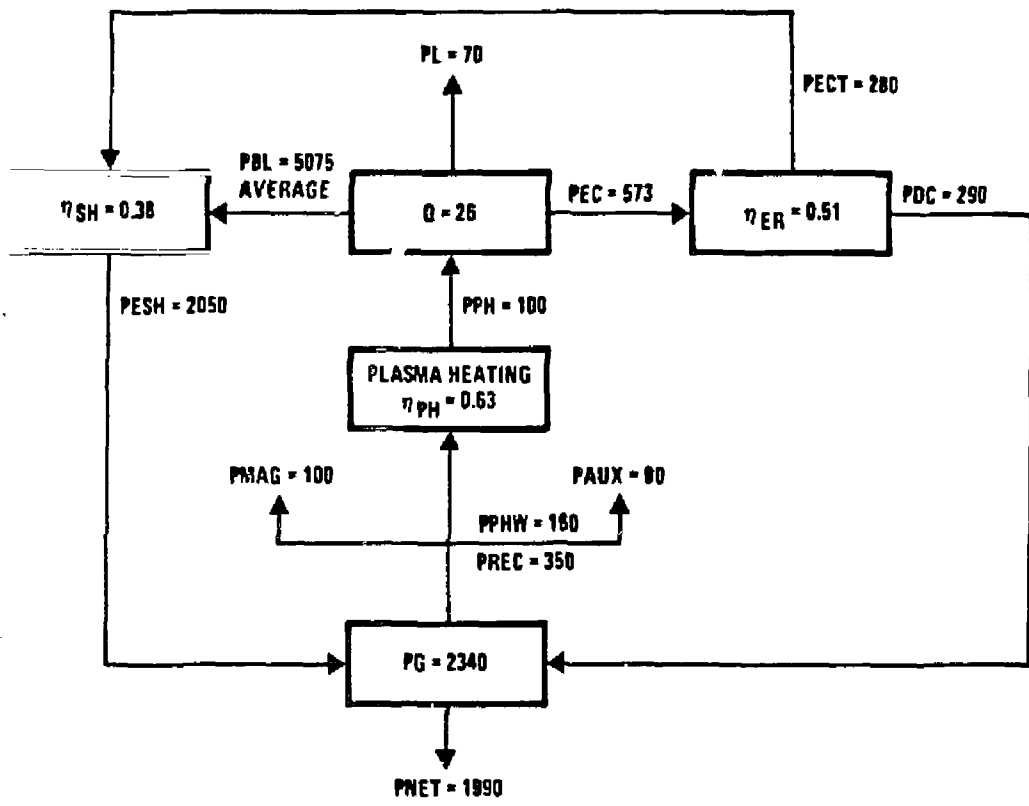


Figure 26.

Fusion Breeder Average Integrated Power Flow Summary

to sustain the 2600 MW<sub>f</sub> plasma. The heating systems require 160 MWe of recirculating power which is added to a 100 MWe power requirement for the copper choke coils and an additional 90 MWe power requirement for auxiliary systems (total recirculating power = 350 MWe)

Of the combined fusion plus heating power (2700 MW total), 70 MW is lost to the system (low grade heat), 573 MW is intercepted by the direct converter, and 2057 MW of neutrons are used to produce an average-over-cycle blanket thermal power of 5075 MW<sub>t</sub> (M<sub>ave</sub> = 2.46). The direct converter produces 290 MWe of power and returns 280 MW<sub>t</sub> of useful lower temperature heat to the thermal power conversion system. This power, combined with the blanket power, and converted to electricity at 38% produces an additional 2050 MWe of power. The net power produced is 1990 MWe. This compares with a MARS power output, using the same fusion plant, of 1200 MWe.

#### IV.C Plant Cost Estimate

A substantial fraction of the MARS effort <sup>(10)</sup> was devoted to the development of direct cost estimates for the various plant components. The reference fusion breeder would utilize the identical fusion plant (i.e., end plugs and many auxiliary systems). Therefore many of the individual MARS subsystem cost estimates are applicable. Cost estimates for subsystems which are not identical to MARS subsystems were developed separately or, if the fusion breeder subsystem was similar to, but larger than the MARS subsystem, but subsystem costs were scaled up relative to the MARS values. Typical scaling exponents were calculated according to the formula

$$C = C_{\text{MARS}} \left( \frac{P}{P_{\text{MARS}}} \right)^n$$

where P is the applicable power level (based upon peak power at end-of-cycle)

and n, the scaling exponent varied between 0.6 and 0.7, depending upon the particular subsystem.

A comparison of the MARS and fusion breeder direct cost estimates by engineering cost account is provided in Table 12. Some notable differences include the following:

- Reactor Building (Acct 21.01)- Cost increased by 55 \$M to provide nuclear grade containment
- Miscellaneous Building (Acct 21.06)- Cost increased by 48 \$M to provide beryllium/thorium fabrication buildings
- Fusion Systems (Acct 22.01)- First wall/blanket/shield and magnet costs increased by 505 \$M to provide larger first wall radius and 253 m<sup>3</sup> of beryllium pebbles at a unit cost of  $8.9 \cdot 10^5$  \$/m<sup>3</sup> (480 \$/Kg)
- Main Heat Transfer Components (Acct 22.02)- Cost increased by 223 \$M to provide higher power and intermediate sodium loop
- Other Plant Equipment (Acct. 22.06)- Cost increased by 442 \$M to provide large coolant dump tanks, dump tank safety systems, the Be/Th fuel handling system, beryllium and thorium fabrication equipment, and a pyro-chemical fuel reprocessing plant.
- Turbine Generator Plant (Acct. 23)- Cost increased by 128 \$M to provide higher power level

Table 12. System Cost Summary  
(10th of a Kind Costs, \$M, 1983)

NUMBER	ACCOUNT TITLE	MARS	FUSION BREEDER
20	Land Acquisition	5	5
21	Structures and Site Facilities	212	331
21.01	Site Improvements and Facilities	11	11
21.02	Reactor Building	87	142
21.03	Turbine Building	36	46
21.04	Cooling System Structures	5	8
21.05	Power Supply and Energy Storage Bldg.	5	5
21.06	Miscellaneous Building (incl. hot cell, tritium processing, beryllium/thorium fabrication)	68	116
21.07	Ventilation Stack	3	3
22	Plant Equipment	1292	2440
22.01	Fusion Systems	893	1398
22.01.01	Blanket and First Wall	71	283
22.01.02	Shield	75	117
22.01.03	Magnets	493	727
22.01.04	Neutral Beam and RF Heating	101	101
22.01.05	Primary Structure and Support	55	72
22.01.06	Vacuum Systems	7	7
22.01.07	Power Supply, Switching, and Energy Storage	63	63
22.01.08	Drift Pump Coils	5	5

Table 12. System Cost Summary (Continued)

NUMBER	ACCOUNT TITLE	MARS	FUSION BREEDER
22.01.09	Direct Converter	23	23
22.02	Main Heat Transfer (incl. Primary loop, pumps, heat exchangers)	237	460
22.03	Cryogenic and Auxiliary Cooling	50	47
22.04	Structure and Coolant Radioactive Waste Treatment	11	12
22.05	Tritium Handling and Storage	46	27
22.06	Other Plant Equipment	30	472
22.06.01	Maintenance Equipment	26	37
22.06.02	Liquid Metal Heating	1	3
22.06.03	Coolant Dump Tanks	3	11
22.06.04	Dump Tank Safety System	--	80
22.06.05	Be/Th Fuel Handling System	--	30
22.06.06	Be Fabrication	--	38
22.06.07	Th Fabrication	--	38
22.06.08	Pyro-Chemical Uranium/Thorium Reprocessing (incl. building)	--	235
22.07	Instrumentation and Control	25	25
23	Turbine Generator Plant	236	364
24	Electric Plant Equipment	138	138
25	Miscellaneous Plant Equipment	28	28
26	Special Materials	126	72
26.01	Liquid Metal Coolant	124	18

Table 12. System Cost Summary (continued)

NUMBER	ACCOUNT TITLE	MARS	FUSION BREEDER
26.02	Beryllium in Process	--	46
26.03	Thorium in Process	--	8
26.04	Other	1	--

- Special Materials (Acct. 26)- Cost decreased by 106 \$M because highly enriched  $^6\text{Li}$  required for Pb-Li coolant in MARS is not used in fusion breeder

As shown in Table 13, the overall direct cost increase for the fusion breeder relative to MARS is estimated to be about 1430 \$M in mid-1985 dollars. Adding 35% for indirect construction costs, 15% for contingency, and assuming 6 and 8 year construction periods for MARS and the fusion breeder, respectively, results in total cost estimates of about 3800 and 6275 \$M for the two plants. Thus, the fusion breeder is estimated to cost about 70% more than the MARS fusion-electric plant, but also would produce about 70% more electricity on average. In addition, the fusion breeder produces about 6660 kg/yr of  $^{233}\text{U}$  (70% capacity factor) - enough fissile fuel to provide makeup for 25 1 GWe LWR reactors!

Table 13. Plant Cost and Performance Comparison  
(\$M 1985)

COST	MARS	FUSION BREEDER
Direct Cost (\$M 1983)	2089	3378
Adjustment to Mid-1985 (7%)	143	236
Adjusted Direct Cost	2182	3614
Indirect Costs (35% of Direct)	764	1275
Contingency (15% of D + I)	442	732
Total Overnight Cost	3387	5611
Construction Time (yr)	6	8
Construction Mode	Private	Government
Cost of Money During Construction	406	667
Total Cost (\$ 1985)	3797	6278
Net Electricity (MW <sub>e</sub> )	1198	1990
Cost Per Unit Elec. (\$/kW <sub>e</sub> )	3169	3154
<sup>233</sup> Production (kg/yr 70% capacity factor)	--	6656

## V. FUEL CYCLE TECHNOLOGIES

The principal role of the fusion breeder reactor is to provide an external source of fissile fuel to support a fission power reactor economy composed of light water reactors (LWRs) or other fission reactors. In this role, the fusion breeder is operationally similar to a fissile enrichment plant which requires no fissile fuel stream and is an electricity producer rather than a consumer. In contrast with fission breeder reactors (i.e., liquid metal fast breeder reactor (LMFR) and light water breeder reactor (LWBR), the neutron rich fusion breeder is a subcritical assembly, produces an order of magnitude more net excess fuel per unit of thermal power, and is not subject to the neutron balance constraints of conventional fission reactors. As a result, a wide variety of fuel cycles and fuel forms are possible.

In this section, several candidate fuel cycle and technology options for fusion breeders and LWR's are briefly reviewed. This review is followed by a more specific discussion relating to the reference fusion breeder fuel cycle. Although not discussed here, a process description and cost estimate for beryllium pebble manufacture/recycling is provide in Reference 2. Conceptual plant designs and costing analysis relating to aqueous (PUREX-/THOREX), pyro-chemical and molten salt fuel reprocessing facilities for the fusion breeder discharge fuel are presented in References 2,6, and 20. Cost estimates for other fuel cycle operations (e.g., tritium removal from lithium) are also provided in Reference 2.

### V.A. Fusion Breeder Fuel Reprocessing Issues

A general schematic of the fusion breeder/fission burner reactor fuel cycle is shown in Figure 27. Several features are deserving of note. Most importantly, the overall fuel cycle is separable into two distinct fuel cycles

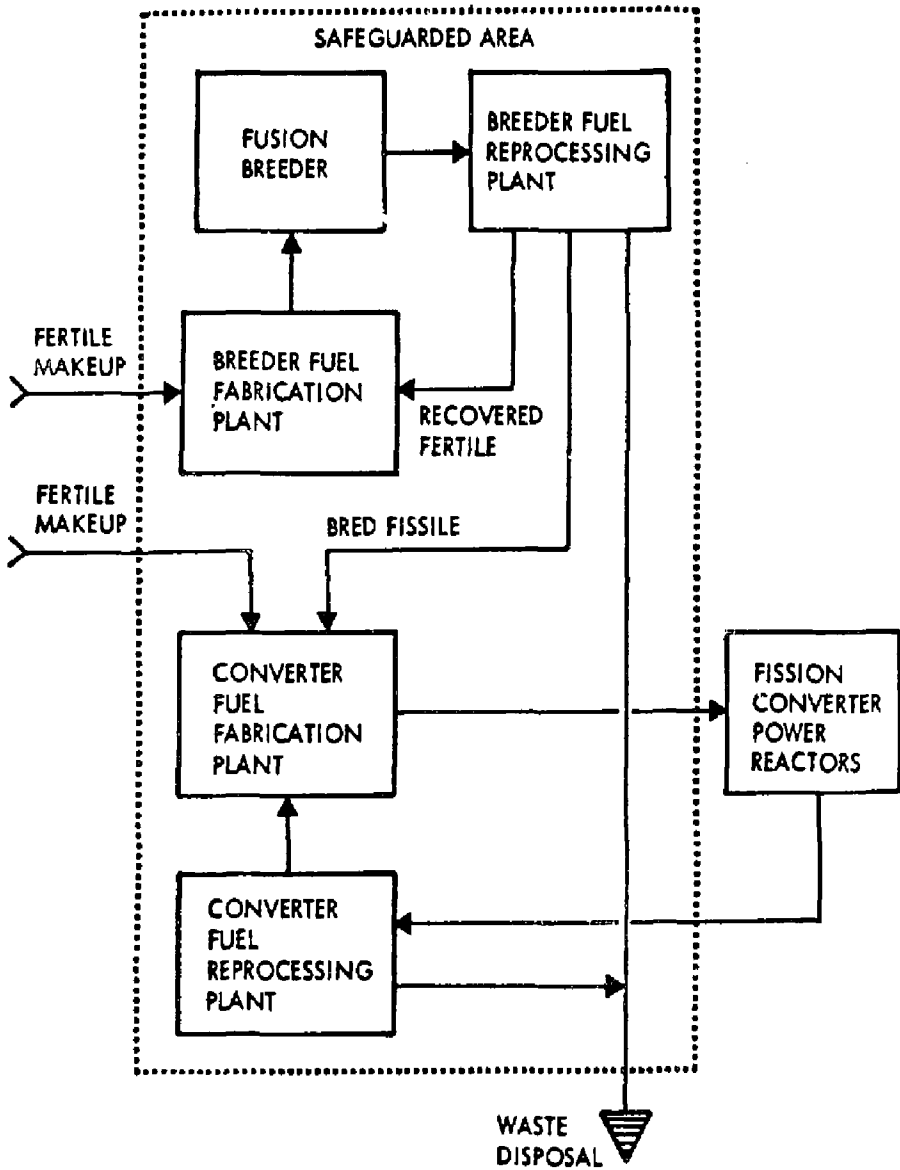


Figure 27.

General Schematic of the Fusion Breeder/Fission  
Burner Reactor Fuel Cycle

which are coupled by the flow of bred fissile material from the fusion breeder to the fission converters. With the exception of issues which bear upon the type of converter fuel fabrication plant required (e.g., the amount of  $^{232}\text{U}$  in the bred  $^{233}\text{U}$ ), the breeder and burner fuel cycles are entirely separable.

Also, both the fusion breeder and fission client fuel cycles are closed by reprocessing and recovery of fissile materials. Although direct enrichment (or "refresh") fuel cycles, which do not employ reprocessing, have been examined in the past, these lead to inefficient fissile production in the fusion breeder as well as the disposal and loss of large quantities of valuable fissile resources. Our results indicate that, like the LMFBR, the fusion breeder requires a closed fuel cycle to achieve adequate economic performance.

In developing the reference fusion breeder concept, two candidate thorium fuel reprocessing technologies have been considered. A key concern regarding the use of a conventional aqueous chemistry (THOREX) fuel reprocessing plant to extract  $^{233}\text{U}$  from thorium metal fuel is cost. In the suppressed fission fusion breeder fuel cycle, fissile fuel is discharged at very low fission burnup ( $\sim 800$  MWD/MTHM) and at very low concentration ( $\sim 1\%$  fissile material in thorium). Low burnup, an advantage, leads to lower radioactivity in the discharged fuel with favorable impact on fuel reprocessing and fabrication processes. The low discharge concentration, leads to high unit costs (i.e., \$/gm) to recover the bred fuel. This situation is illustrated in Table 14, which shows typical reprocessing cost data allowing a comparison of the cost to recover fissile fuel using the THOREX and a pyro-chemical reprocessing options. It is important to note that a typical  $^{233}\text{U}$  production cost not including reprocessing is 50 \$/g. Therefore, THOREX reprocessing could account for as much as 1/2 of the cost of bred fuel. It should also be noted

that the thorium throughputs shown in Table 14 are applicable to full scale reprocessing plants that each process output of three fusion breeders.

In comparison with the aqueous fuel reprocessing technologies, the more compact pyro-chemical fuel reprocessing technology for thorium metal fuels is expected to result in a more tolerable contribution to the cost of bred fissile fuel. Although the development program required to assure the feasibility of this technology is more of a concern, the pyro-chemical reprocessing technology offers an economic incentive in the range of 100 \$M/yr-a strong motivation for development.

#### V.B. Overview of LWR Fuel Cycles and Issues

Light water moderated power reactors are expected to dominate nuclear power production in the 2020 timeframe when the fusion breeder reactor could become commercially available. Consequently, the LWR is considered as the principal type of fission client reactor, but the discussion is also applicable to more advanced fission converters (modular HTGR, etc.). The cores of these reactors would be modified to provide passive safety or increased fuel economy, but fissile makeup and inventories will continue to be required.

If the fuel bred in the fusion breeder is  $^{233}\text{U}$ , three fuel cycle options (30,31) are available:

- The thorium fuel cycle (typically 3.4%  $^{233}\text{U}$ , 96.6%  $^{232}\text{Th}$ )
- The denatured thorium fuel cycle (typically 3.3%  $^{233}\text{U}$ , 18%  $^{238}\text{U}$ , 78.7%  $^{232}\text{Th}$ )
- The denatured uranium fuel cycle (typically 2.4%  $^{233}\text{U}$ , 97.6%  $^{238}\text{U}$ )

Among these, the thorium fuel cycle is most efficient with respect to fissile

Table 14. Typical Reprocessing Economics  
(1985 \$)

	THOREX	PYRO-CHEMICAL
Throughput (MT/yr) <sup>a</sup>	1900	1900
Fissile discharge, assy, atom %	1.05	1.05
Plant capital cost, \$M	3000	1500
Cost of capital, \$M/yr <sup>b</sup>	393	197
Plant operating cost, \$M/yr <sup>c</sup>	172	40
Total annual cost, \$M/yr	565	237
Reprocessing cost, \$/kgHM	297	125
Unit cost, \$/g	28.3	11.9

- a) Three fusion breeders sharing a reprocessing plant
- b) Utility ownership (13.1%/yr)
- c) First year, increases 3%/yr thereafter

feed requirements, but the denatured fuel cycles provide some isotopic dilution, and have intrinsic proliferation resistance.

Both the thorium and denatured thorium LWR fuel cycles will require THOREX fuel reprocessing plant technology as well as a remote and shielded fuel fabrication technology. These technologies have not yet been developed to commercial scale and, although technically straightforward, both processes are expected to result in comparatively high costs per unit of heavy metal throughput. The denatured uranium fuel cycle requires 28% more fissile feed than the denatured thorium fuel cycle, but is compatible with the more developed PUREX reprocessing technology.

It is important to note that some plutonium burners might be used even if  $^{233}\text{U}$  is bred in the fusion breeder. That is, both the denatured thorium fuel cycle and the denatured uranium fuel cycle produce appreciable quantities of plutonium in the  $^{233}\text{U}$  fueled LWRs (30,31). This is a result of neutron absorption in  $^{238}\text{U}$  with subsequent conversion to fissile plutonium. The fissile plutonium can be disposed by recovery and recycle in "secondary" plutonium burning LWRs which might be located with the fusion breeders within the safeguarded fuel cycle centers.

The LWR fuel cycle performance data used in the analysis provided in Section V.C and in Section VI is summarized in Table 15. In this table, six LWR fuel cycles are presented. The first, for a plutonium burner, applies to the LWRs which would be used to burn excess plutonium produced in  $^{233}\text{U}$  burners which use  $^{238}\text{U}$  as fertile material. The second and third fuel cycles, described earlier, would each consume  $^{233}\text{U}$  feed and produce some excess plutonium. The fourth fuel cycle is a combination of the first and second case, (74%  $^{233}\text{U}$  burners, 26% Pu burners) such that all fissile material is recycled. The fifth fuel cycle combines the first and third fuel cycles

Table 15. LWR Fuel Cycle Performance Data

	LWR FUEL CYCLE TYPE					
	Pu Burner	Denatured Uranium (DU)	Denatured Thorium (DT)	DU + Pu (a)	DT + Pu (b)	<sup>235</sup> U Burner
Net Fissile Requirement, g/KW-yr (c)	0.250	0.205	0.144	0.153	0.126	0.194
Excess Plutonium Production, g/KW <sub>t</sub> -yr(c)	none-recycled	0.068	0.028	none-recycled	none-recycled	none-recycled
Fuel Burnup, MWD/MTHM	30,400	33,000	33,400	32,300	33,000	30,400
Equilibrium Fissile Enrichment, atom %	4.9	2.4	3.3	3.1	3.5	3.2
Core Power Density, kW <sub>t</sub> /KgHM	37.1	37.2	40.2	37.2	39.8	38.4
Equilibrium Fissile Inventory, g/KW <sub>t</sub>	1.83	0.68	1.09	1.07	1.29	1.14
Net Thermal-to-Electric Efficiency, %	33.4	33.4	33.4	33.4	33.4	33.4

a) mixed system includes 74% denatured uranium fuel cycle LWRs and 26% plutonium fuel cycle LWRs

b) mixed system includes 88% denatured thorium fuel cycle LWRs and 12% plutonium fuel cycle LWRs

c) at 100% plant capacity factor

similarly (88%  $^{233}\text{U}$  burners, 12% Pu burners).

Finally, the sixth fuel cycle applies to an LWR which uses mined uranium and recycles both the remaining uranium at end-of-cycle and the bred plutonium. This fuel cycle was used to compare the cost of electricity for a conventionally fueled LWR (i.e., mined uranium) with that of a symbiotic fusion-fission system (fifth fuel cycle in Table 15). The analysis is presented in Section VI.

#### V.C Symbiotic Electricity Generation Systems

It is of interest to explore the typical size and characteristics of a fuel cycle center which contains fusion breeders, their fuel cycle facilities, and the fuel cycle facilities associated with a self-consistent number of client LWRs. The size of such a fuel cycle center will be determined by two constraints:

- All fuel cycle facilities should be large enough to benefit from economies of scale
- The total number of fuel cycle centers should be small (perhaps 5-10 in the U.S.)

A fuel cycle center concept for the reference fusion breeder with LWR denatured thorium (and secondary plutonium) fuel cycle clients is shown in Figure 28. In this configuration, three fusion breeders supply about 20,000 Kg/yr of  $^{233}\text{U}$  (70% capacity factor) to support 75 1 GWe LWR clients for a total electrical output of about 81 GWe. The plutonium produced by 66 of the LWRs is sufficient to support an additional 9 1 GWe LWRs. The fusion breeders each have a dedicated beryllium recycle plant and, together share a single pyrochemical fuel reprocessing plant of 1902 MT/yr capacity. The mixed oxide LWR reprocessing/fabrication throughout is about 1675 MT/yr. Of this, about

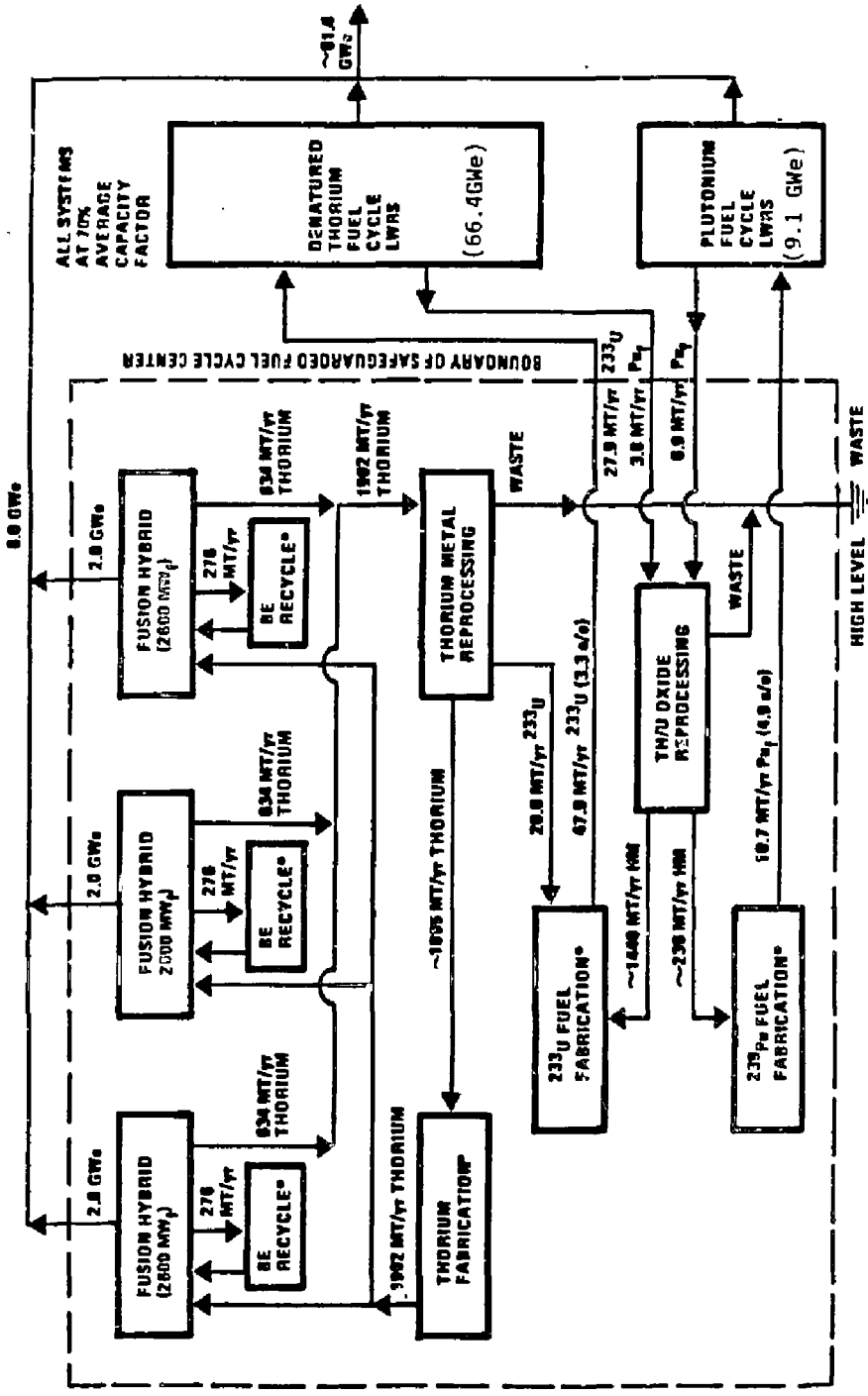


Figure 28.  
 A Symbiotic Electricity Generation System Based upon a  
 Denatured Thorium Fuel Cycle

235 MT/yr is associated with the plutonium burners (PUREX reprocessing) and about 1440 MT/yr is associated with the  $^{233}\text{U}$  burners, (THOREX reprocessing). It is anticipated that low level wastes generated in the reprocessing and fuel fabrication facilities would be disposed on-site, but that high level wastes would be shipped elsewhere for permanent disposal.

A similar fuel cycle center concept, where LWR denatured uranium fuel cycle clients, are utilized instead of denatured thorium fuel cycle clients has also been considered. In this case a smaller total of about 62 LWRs can be supported (including about 16 plutonium burners), but since none of the LWR fuel is thorium oxide based, the need for THOREX reprocessing of LWR fuel is eliminated and PUREX reprocessing can be used. The net electrical output for this alternative system would be 68 GWe, a 16% decrease.

## VI. ECONOMICS

In this section, the results of two models of the economic performance of the symbiotic shown in Figure 28 are reviewed. The symbiotic system is also compared with a conventional LWR fuel cycle ( $^{235}\text{U}$  Burner of Table 15) to determine the "indifference", or "breakeven" cost of  $\text{U}_3\text{O}_8$ . When the market cost of mined  $\text{U}_3\text{O}_8$  reaches the breakeven cost, the fusion breeder is expected to provide an economic benefit.

### VI.A System Average Capital Cost Model

All of the economic models of symbiotic electricity generation systems share a common feature: they recognize that including the fusion breeders and all of the client LWRs, only one product, electricity, is produced. The first and most simple model attempts to estimate and compare the average capital cost (per unit electricity generation) of the symbiotic system with that of an LWR alone. This model ignores all fuel cycle facilities and fissile inventory charges, but provides an excellent measure of the dominant features of the system. In this model, the average capital cost, in LWR units is

$$\text{ACC} = \frac{(1 \times C^F) + (R_t \times 1)}{(1 \times \eta_{\text{rel}}) + (R_t \times 1)} = \frac{C^F + R_t}{\eta_{\text{rel}} + R_t}$$

where  $C^F$  is the fusion breeder cost relative to the LWR cost (basis:  $\$/\text{KW}_t$ ),  $R_t$  is the fusion breeder thermal support ratio and  $\eta_{\text{rel}}$  is the relative thermal efficiency of the fusion breeder relative to the LWR.

For example, the fusion breeder cost (not including its pyro-chemical reprocessing plant or other fuel cycle facilities) is 5596  $\$/\text{MW}_t$  and its average thermal power is 5600  $\text{MW}_t$ . Its cost relative to a 1 GWe, 1330  $\$/\text{MW}_t$  LWR of 3000  $\text{MW}_t$  power,  $C^F$ , is  $(5596/5600) / (1330/3000) = 2.25$ . The fusion breeder

produces 6656 Kg/yr of  $^{233}\text{U}$  and the LWR requires 265 Kg/yr. The thermal support ratio,  $R_t$ , is  $(6656/5600) / (265/3000) = 13.5$ . The fusion breeder produces 1990 MWe, so the relative thermal efficiency,  $\eta_{rel}$ , is  $(1990/5600) / (1000/3000) = 1.07$ . Substituting these values into the above equation gives  $ACC = 1.08$ , indicating that the cost of providing fissile makeup for LWRs in a symbiotic system is roughly equivalent to increasing the capital cost by only 8%.

## VII.B Higher Level Economics Modeling

### VII.B.1 Discussion

The next level of detail in economics analysis considers the following additional aspects of the symbiotic electricity generation system:

- Inflation (3%/yr) over the plant lifetime (30 years).
- Capital and operating costs associated with fuel cycle operations.
- Typical utility or government financing of the capital costs.
- Anticipated escalations in operating costs.
- Fissile inventory carrying charges.

The methodology used to perform the analysis is incorporated into a TRW Systems modeling code (PERFEC) and is described in detail in Reference 2.

A key feature is that a year-by-year cost balance is performed such that the cost of electricity and fissile fuel produced by the fusion breeder are identical to the cost of electricity produced and the cost of fuel consumed by the client LWRs in the same year. Thus, fuel revenues and costs exactly cancel within the system and, as discussed earlier, the only net product from the symbiotic system is electricity. The method provides a year-by-year cost

of electricity which reflects the overall capital, operating, and fissile inventory charges of the symbiotic system.

A second feature of the PERFEC model is that it allows a year-by-year comparison with an alternative LWR fuel cycle in which the fissile feed comes from mined  $U_3O_8$ . Three types of comparison are of interest:

- year one breakeven price of  $U_3O_8$ .
- 30 year breakeven price of  $U_3O_8$ .
- 30 year integrated benefit.

In the first comparison, the required price of  $U_3O_8$  (in 1985 dollars) such that the fusion-fission system provides electricity at the same cost as the  $U_3O_8$ - fueled LWR in the first year operation is calculated. When the actual market price of  $U_3O_8$  (again, in 1985 dollars) reaches this level, the fusion breeder becomes economical in the first year.

If, in later years, the cost of  $U_3O_8$  increases with inflation, then the comparison becomes increasingly favorable to the symbiotic system during the second and later years. The second of the above comparisons, determines a lower year one cost of  $U_3O_8$  that, inflated in each of 30 years, provides a zero net benefit over the entire period. Thus, the 30 year breakeven cost of  $U_3O_8$  does not provide breakeven in the first year (the fusion breeder loses revenue), but the discounted present value of excess revenues exceed breakeven during the second half of the thirty year period by enough to compensate for early losses.

The third type of comparison is intended to evaluate the present value of a thirty year net benefit (or loss) starting with a user input cost of  $U_3O_8$  in year one and assuming a  $U_3O_8$  escalation rate (e.g., 55 \$/Kg and 3%/yr). If

the calculated year one breakeven cost is input, the 30 year integrated benefit is expected to be very large because of a positive cash flow beginning in the second year. Conversely, if the 30 year breakeven cost is input, the 30 year benefit is, by definition, zero.

### VII.8.2 U<sub>3</sub>O<sub>8</sub> Fueled LWR

Before performing such comparisons, it is of interest to define and evaluate U<sub>3</sub>O<sub>8</sub> fueled LWRs (Table 15) and their fuel cycle costs. Typical cost data for such LWRs is provided in Table 16. The LWR capital and fuel cycle cost estimates were developed using References 30 and 32, but have been modified to account for inflation to 1985 and other factors (such as a prorated contribution for the secondary plutonium burners). It should be noted that reasonably cost effective fuel reprocessing and fabrication plants are assumed to exist. It should also be noted that the assumed cost of enrichment (60 \$/Kg SWU) is less than half the current cost. It is expected that less expensive enrichment processes (e.g., laser isotope separation or plasma isotope separation) will become available.

As indicated in the table, if the price of U<sub>3</sub>O<sub>8</sub> does not increase beyond a nominal value of 55 \$/Kg (which is near today's price), the cost of electricity for the U<sub>3</sub>O<sub>8</sub> fueled LWR is expected to be 52 mil/KW<sub>e</sub>H in the first year. The average present value of the electricity cost, 33 mil/KW<sub>e</sub>H, is lower because the present value of the annual cost of plant capital decreases year-by-year due to the assumed 3% inflation rate.

Table 16. Economics Results For a  $U_3O_8$  Fueled LWR With Reprocessing

---

LWR Capital Cost ( $\$/kW_t$ )	444
Total Fixed Charge Rate (%/yr)	13.2
Fuel Cycle	Full Recycle
$^{233}U$ Consumption ( $g/kW_t\text{-yr}$ )	0.194
Average Burnup (MWD/MTHM)	30,400
Reprocessing Cost ( $\$/kgHM$ )	417
Fabrication Cost ( $\$/kgHM$ )	685
Enrichment Cost ( $\$/kg$ separative work)	60
Transport and Disposal Cost ( $\$/kgHM$ )	260
Year One Price of Purchased $U_3O_8$ ( $\$/kg$ )	55
Year One Cost of Electricity ( $mil/kW_eH$ )	52
$U_3O_8$ Escalation Rate (%/yr)	3
Average PV Cost of Electricity ( $mil/kW_eH$ )	33

### VII.B.3 Economics Results for the Symbiotic System

Economics results for the symbiotic electricity generation system depicted in Figure 28 are shown in Table 17. Two cases are provided. In the first, the fusion breeder is government owned (similar to uranium enrichment plants today), while in the second, the fusion breeder is utility owned. Although it is unlikely that a single utility would own a fusion breeder that supports ~ 25 GWe of LWR capacity, a consortium of utilities might undertake such an investment.

The government ownership case offers several attractive features - especially for the first several fusion breeders. Specifically, the government is better equipped to control and account for the produced fissile material, thus providing assurance that the possibilities for diversion of vulnerable fissile materials from the fuel cycle center will be minimized. Also, the government does not pay taxes and its cost of capital is only about half that of private utilities (see Table 17).<sup>a</sup>

This large advantage translates to an even greater advantage in the cost of fissile fuel because the cost of electricity, which is dominated by the LWR capital and operating cost, is relatively stable regardless of fusion breeder ownership (Table 17). After electricity revenues are subtracted from the government's fusion breeder total annual cost, the balance is so small that divided by the annual fissile fuel production, a year one <sup>233</sup>U cost of only 2.6 \$/g might be achieved. This compares with a 59 \$/g fissile fuel cost for the utility ownership case, in which roughly half of the fusion breeder total annual cost must be compensated by fissile fuel sales.

---

a) It should be noted that savings attributed to government ownership result from uncollected tax revenues that would otherwise be paid by a private operator

Table 17. Economics Results for the Symbiotic System

FUSION BREEDER OWNER/OPERATOR	CASE 1 GOVT	CASE 2 UTILITY
Fusion Breeder direct cost (\$/kW <sub>t</sub> )	604 604	
Fusion Breeder total cost (\$/kW <sub>t</sub> )	1015 1121	
Total fixed charge rate on fusion breeder plant capital (%/yr)	6.3 13.1	
Fusion Breeder capital cost (\$/kW <sub>t</sub> -yr)	64.2 147	
Fusion Breeder operating cost (\$/kW <sub>t</sub> -yr)	34.0 34.0	
Fusion Breeder fissile inventory cost (\$/kW <sub>t</sub> -yr)	0.2 13.6	
Fusion Breeder total annual cost (\$/kW <sub>t</sub> -yr)	98 195	
LWR OWNER/OPERATOR	UTILITY	UTILITY
LWR direct cost (\$/kW <sub>t</sub> )	250 250	
LWR total cost (\$/kW <sub>t</sub> )	444 444	
Total fixed charge rate on LWR plant capital (%/yr)	13.2 13.2	
LWR annual capital cost (\$/kW <sub>t</sub> -yr)	58.6 58.6	
LWR annual operating cost (\$/kW <sub>t</sub> -yr)	30.1 30.1	
LWR annual fissile inventory cost (\$/kW <sub>t</sub> -yr)	0.5 11.9	
Hybrid capital cost/LWR capital cost	2.29 2.53	
Hybrid annual cost/LWR annual cost	1.10 1.93	
	100	

Table 17. Economics Results for the Symbiotic System (cont'd)

	Case 1	Case 2
Year one cost of LWR electricity (\$/kW <sub>e</sub> H)	0.044	0.047
Year one cost of <sup>233</sup> U (\$/g)	2.6 58.8	
Year one breakeven cost of U <sub>3</sub> O <sub>8</sub> (\$/kg)	15.7 289	
30-year average present value cost of LWR	0.032	0.036
Year one cost of U <sub>3</sub> O <sub>8</sub> for 30-year breakeven (\$/kg)	13.1 196	
Integrated benefit assuming 55 \$/kg U <sub>3</sub> O <sub>8</sub> cost in year one (\$/kW <sub>t</sub> )	1227 -4129	
Integrated benefit as ratio of total breeder cost (%)	121 -368	

As shown in the table, for government ownership, the year one breakeven price of  $U_3O_8$  is only about 16 \$/Kg, or about 1/3 of the current price. Assuming that the mined uranium price is 55 \$/Kg, the government owned fusion breeder would provide an integrated benefit of about 1230 \$/KW<sub>f</sub>, or about 7 \$ billion over 30 years!

For utility ownership, the year one  $U_3O_8$  breakeven price of about 290 \$/Kg is considerably higher than the currently depressed price of uranium. However, this price is not inconsistent with prices based upon projected mined uranium forward costs for the 2020-2040 timeframe (30), which assume that nuclear power develops an increasing share of the electricity generation market and that the uranium price/cost ratio exceeds about 1.5 (historically closer to 2). Finally, it should be noted that the difference in year one  $^{233}U$  costs between the government and utility ownership cases, about 56 \$/g, translates to only a 2.3 mil/KWe LWR electricity cost difference! Thus, even a utility owned fusion breeder can place a very reasonable upper bound on the cost of LWR electricity, as well as on the cost of mined  $U_3O_8$  and the allowed cost of competitive technologies (such as fusion-electric power generation and the LMFBR).

### VIII. Research Needs

Several experimental programs should be implemented to confirm the viability of the reference fusion breeder, exclusive of the fusion plasma confinement technology. A brief list of high priority research areas follows:

- MHD Pressure Drops- packed bed and duct flow including electrical insulator development
- Liquid Metal Compatibility- Intermettalic reactors, mass transfer, fission product/actinide transport, coatings development
- Beryllium Irradiation Damage- Irradiation creep, pebble failure modes
- Pyro-chemical Reprocessing Magnesium dissolution process demonstration
- Fissile Breeding- Integral test assembly with a point neutron source
- Pebble Flow- Sub-scale mockup

## IX. REFERENCES

1. C. Max, "Uranium Resources and the Development of Fission and Fusion Breeder Reactors," UCRL-52000-84-10, Energy and Technology Review, Lawrence Livermore National Laboratory (1984).
2. D. H. Berwald, et al., "Fission Suppressed Hybrid Reactor - The Fusion Breeder," UCID-1963-19638, Lawrence Livermore National Laboratory (1982).
3. R. W. Moir, et al., "Helium Cooled Molten-Salt Fusion Breeder," UCID-20153, Lawrence Livermore National Laboratory (1984).
4. R. W. Moir, et al., "Feasibility Study of a Fission-Suppressed Tokamak Fusion Breeder," UCID-20154, Lawrence Livermore National Laboratory (1984).
5. "Special Topics Reports for the Reference Tandem Mirror Fusion Breeder," UCID-20166, Lawrence Livermore National Laboratory -
  - Volume 1: T. J. McCarville, et al., "Liquid Metal MHD Pressure Drop Effects in the Packed Bed Blanket," September, 1984.
  - Volume 2: I. Maya, et al., "Reactor Safety Assessment," September, 1984.
  - Volume 3: L. Miller, et al., "Beryllium Lifetime Assessment," October, 1984.
  - Volume 4: G. Orient, et al., "Structural Analysis," December, 1984.
  - Volume 5: J. D. Lee and B. R. Bandini, "Neutronic Issues and Optimization," March, 1985.
6. J. D. Lee, Ed., "Feasibility Study of a Fission Suppressed Tandem Mirror Hybrid Reactor," Lawrence Livermore National Laboratory, UCID-19327 (1982).
7. R. W. Moir, et al., "Fusion Breeder Program Interim Report", December 1981 - February 1982," Lawrence Livermore National Laboratory, UCID-19406-1 (June 1982).
8. C. Wong, et al., "Measurements and Calculations of the Leakage Multiplication from Hollow Beryllium Spheres," Fusion Technology, 8, 1165 (1985).
9. T. J. McCarville, et al., "Technical Issues for Beryllium Use in Fusion Blanket Applications," UCID-20319, Lawrence Livermore National Laboratory (1985).
10. B. G. Logan, et al., "MARS - Mirror Advanced Reactor Study," UCRL-53480, Lawrence Livermore National Laboratory (1984).

REFERENCES (continued)

11. C. C. Baker, et al., "STARFIRE - A Commercial Tokamak Fusion Power Plant Study," ANL/FPP-80-1, Argonne National Laboratory (1980).
12. L. J. Perkins, et al., "Plasma Engineering for MINIMARS: A Small Commercial Tandem Mirror Reactor with Octupole Plugs," Fusion Technology, 8, 685 (1985).
13. J. Sheffield, et al., "Cost Assessment of a Generic Magnetic Fusion Reactor," TM-9311, Oak Ridge National Laboratory (1985).
14. D. L. Chapin, et al., "Preliminary Feasibility Assessment of Fusion-Fission Hybrids," WFPS-TME-81-003, Westinghouse Fusion Power Systems Department (1981).
15. R. P. Rose, et al., "Design Study of a Fusion-Driven Tokamak Hybrid Reactor for Fissile Fuel Production," ER-1083, Electric Power Research Institute (1979).
16. D. L. Smith, et al., "Blanket Comparison and Selection Study - Final Report," ANL/FPP-84-1, Argonne National Laboratory (1984). See also M. A. Abdou, et al., "Blanket Comparison and Selection Study - Interim Report," ANL/FPP-83-1, Argonne National Laboratory (1983).
17. D. Pachur, "The Influence of Neutron Fluence and Irradiation Temperature on the Radiation Annealing Mechanisms of Reactor Pressure Vessel Steels," ANS Trans., 38, 306 (1981)
18. W. F. Calaway, "Electrochemical Extraction of Hydrogen from Molten LiF-LiCl-LiBr and Its Application to Liquid Lithium Fusion Reactor Blanket Processing," Nucl. Tech., 39, 63 (1978).
19. V. A. Maroni, et al., "Some Preliminary Consideration of a Molten Salt Process to Remove Tritium from Liquid Lithium Fusion Reactor Blankets," Nucl. Tech., 25, 83, (1975).
20. M. S. Coops and J. B. Knighton, "Recovery of Uranium-233 from a Thorium Breeding Blanket by Pyrochemical Techniques," UCJD-19623, Lawrence Livermore National Laboratory (1982).
21. S. Taczanoski, "Neutron Flux Shaping in Hybrids for Spent Fuel Regeneration Without Reprocessing," proc. of the Third Intl. Conf. on Emerging Nuclear Energy Systems, Helsinki, Finland (1983).
22. R. J. Micklich, "Resonance Self-Shielding Effects in a Combined Tritium and Fissile Breeding Blanket," Trans. Am. Nucl. Soc., 46, 254 (1984).
23. W. R. Meier, "A High Performance, Suppressed-Fission ICF Hybrid," UCRL-89274, Lawrence Livermore National Laboratory (1983).

REFERENCES (continued)

24. W. W. Engle, "ANISN-Multigroup One Dimensional Discrete Ordinates Transport Code with Anisotropic Scattering," RSIC-CCC-254, Oak Ridge National Laboratory (1973).
25. R. E. Macfarlane, "MATX56: A 80 x 24 Library from ENDF/B-5," Los Alamos National Laboratory (1984).
26. E. F. Plechaty and J. R. Kimlinger, "TARTNP: Coupled Neutron-Photon Monte Carlo Transport Code," UCRL-50400, Vol. 14, Lawrence Livermore National Laboratory, (1975). See also C. E. Cullen, "Bondarenko Self-Shielded Newton Cross Sections and Multiband Parameters Derived from the LLNL Evaluated-Nuclear-Data Library (ENDL)," UCRL-50400, Vol. 20, Lawrence Livermore National Laboratory, 1978.
27. E. F. Plechaty, D. E. Cullen, E. J. Howerton, and J. R. Kimlinger, "Tabular and Graphical Presentation of 175 Neutron-Group Constants Derived from the LLNL Evaluated-Nuclear-Data Library (ENDL)," UCRL-50400, Vol. 16, Rev. 2, Lawrence Livermore National Laboratory (1978).
28. G. A. Carlson, "Magnetohydrodynamic Pressure Drop of Lithium Flowing in Conducting Wall Pipe in a Transverse Magnetic Field - Theory and Experiment," Proceedings of the 1st Topical Meeting on the Technology of Controlled Nuclear Fusion, CONF-740402-P1, 1974.
29. D. H. Berwald and S. Zenczak, "Assessment of Beryllium Resources for Fusion Applications," Fusion Technology, B, 1143 (1985).
30. Nonproliferation Alternative Systems Assessment Program (NASAP), DOE/NE-0001, U.S. DOE (1980).
31. Y. I. Chang, et al., "Alternative Fuel Cycle Options: Performance Characteristics and Impact on Nuclear Power Growth Potential," ANL-77-70, Argonne National Laboratory (1977).
32. "Nuclear Energy Cost Data Base, A Reference Data Base for Nuclear and Coal Fired Power Generation Cost Analysis," DDE/NE-0044/2, U.S. Department of Energy (1984).